

## **Internal World Models as Imagination Networks in Cognitive Agents**

Saurabh Ranjan and Brian Odegaard

Department of Psychology, University of Florida

### **Author Note**

ORCID:

Saurabh Ranjan: <https://orcid.org/0000-0002-7868-7223>

Brian Odegaard: <https://orcid.org/0000-0002-5459-1884>

Address Correspondence to:

Saurabh Ranjan: [ranjan.saurabh@outlook.com](mailto:ranjan.saurabh@outlook.com)

Brian Odegaard: [bodegaard@ufl.edu](mailto:bodegaard@ufl.edu)

Competing interests: No competing interests to declare.

Author Contributions:

S.R.: Conceptualization, Visualization, Software, Methodology, Formal analysis, Data curation,  
Writing – original draft, Writing – review & editing.

B.O.: Writing – review & editing, Supervision.

Funding: S.R. was supported by the Threadgill Dissertation Fellowship from the University of Florida for this work.

Code and Data Availability: Code and data will be made public upon publication.

### Abstract

The computational role of imagination remains debated. While classical accounts emphasize reward maximization, emerging evidence suggests imagination serves a broader function: accessing internal world models (IWMs). Here, we employ psychological network analysis to compare IWMs in humans and large language models (LLMs) through imagination vividness ratings. Using the Vividness of Visual Imagery Questionnaire (VVIQ-2) and Plymouth Sensory Imagery Questionnaire (PSIQ), we construct imagination networks from three human populations (Florida, Poland, London; N=2,743) and six LLM variants in two conversation conditions. Human imagination networks demonstrate robust correlations across centrality measures (expected influence, strength, closeness) and consistent clustering patterns, indicating shared structural organization of IWMs across populations. In contrast, LLM-derived networks show minimal clustering and weak centrality correlations, even when manipulating conversational memory. These systematic differences persist across environmental scenes (VVIQ-2) and sensory modalities (PSIQ), revealing fundamental disparities between human and artificial world models. Our network-based approach provides a quantitative framework for comparing internally-generated representations across cognitive agents, with implications for developing human-like imagination in artificial intelligence systems.

*Keywords:* imagination, internal world model, vividness, network science, artificial intelligence

### **Internal World Models as Imagination Networks in Cognitive Agents**

Imagination is the ability to generate internal representations without external information<sup>1-3</sup>, and results in mental simulations which guide learning<sup>4</sup>, planning<sup>2,5-7</sup>, and hypothesis generation<sup>8,9</sup>. Imagination also aids curiosity<sup>10,11</sup> and reasoning<sup>12-15</sup>, helping agents behave in advantageous ways as they interact with external environments. Different forms of imagination have been proposed, including reproductive imagination, which relies primarily on past information and experiences, and productive imagination, which can involve hypothetical or impossible scenarios (e.g., imagining an eight-legged dog)<sup>16</sup>. Thus, imagination has been shown to be involved in various cognitive processes. However, despite its contributions to cognition and behavior, the functional role of imagination remains unclear at present.

One hypothesis is that imagination plays a key role in reinforcement learning, which can improve adaptive behaviors in complex environments. For example, imaginative computations have recently been incorporated into reinforcement learning (RL)-based artificial intelligence (AI), primarily using Monte Carlo tree search methods<sup>7,17-19</sup>. These studies demonstrate how generating internal representations can help AI agents better predict future actions and learn human-like reward-action mappings, resulting in task performance that is equal to or better than humans<sup>17,20-25</sup>. Imagination in the RL framework is utilized for reward maximization<sup>18,23,24</sup>, but critically, evidence shows that imagination does not always lead to optimal reward-seeking behaviors in a task. For instance, in a two-stage choice task, it has been demonstrated that asking participants to imagine pathways to earn terminal rewards did not result in participants choosing optimal solutions<sup>26</sup>. While these behaviors were accounted for by a forgetting parameter in their RL model, one alternative explanation is that imagination (rather than forgetting) led to an increase in the willingness of participants to take risks, which caused suboptimal outcomes<sup>27-29</sup>.

Further evidence that imagination may fail to maximize rewards is found in other studies, which have shown that when monetary incentives are provided to participants to track an object's timing, imagination does not result in better performance<sup>30</sup>. Overall, since humans can engage in activities like creativity, dreaming, and mind-wandering without being motivated by explicit rewards<sup>31-33</sup>, it appears that any account of imagination based solely on reward maximization may be incomplete.

If imagination does not necessarily lead to reward maximization, is there another way to account for its functional role? A large body of work in cognitive neuroscience suggests that imagination reflects simulation from an internal generative model of the world. According to the constructive episodic simulation hypothesis, remembering the past and imagining the future relies on a common system that flexibly recombines episodic details into simulated events<sup>34-36</sup>. Scene construction accounts similarly propose that hippocampal-cortical networks support the generation of coherent, spatially organized scenes that underlie both episodic recollection and fictitious imagination<sup>37-39</sup>. Episodic future thinking research shows that such simulations guide decision-making and planning<sup>40</sup>. From this perspective, the functional role of imagination is to access and deploy an internal world model - a generative representation that supports constructing, evaluating, and comparing possible situations.

Recently proposed *hierarchical* and *heterarchical models of imagination*<sup>41-43</sup> build upon these accounts, arguing that imagination involves semantic memory, episodic memory, attention, and working memory, utilizing domain-preferring brain areas that are bridged *heterarchically* by the domain-general fusiform imagery node (FIN) and *hierarchically* by parietal regions. Recent theoretical work in cognitive neuroscience posits that these heterarchical systems that model reality may be needed to truly understand language and the world itself<sup>44</sup>. Relatedly, in artificial

intelligence research, it has been proposed that imagination’s role is to access the “world model” that a deep-learning model would have learned from the training data<sup>22</sup>. But to date, it remains unclear what the representational properties of such an internal world model actually are, and whether humans and AI models have similar representational characteristics.

In the current work, we ground the world model as structural relationships between imagined items based on long-term memories that are accessed during imagination to report vividness ratings about different scenarios. If imagination consists of simulations drawn from an internal world model, then the pattern of dependencies among imagined scenarios provides an observable signature of (at least part of) a world model’s structure. In humans, vividness ratings are a robust trait that can explain individual differences of a broad range of subjective experiences<sup>45</sup>. But how vividness ratings are associated across different imagined experiences yet remains to be investigated. Human imagination is often evaluated using questionnaires such as the Vividness of Visual Imagery Questionnaire (VVIQ-2)<sup>46</sup> and the Plymouth Sensory Imagery Questionnaire (PSIQ)<sup>47</sup>. While the former uses different environmental scenes, the latter utilizes imagination across different sensory domains. Since both of these questionnaires are text-based, they can be easily applied to various LLM models, allowing for comparisons between human and AI imagination.

In this study, we introduce imagination networks for two questionnaires (the VVIQ-2, and the PSIQ) to compare representations of IWMs in both humans and AI agents. The act of imagining different scenarios likely accesses shared representational content, processing demands, or underlying neural substrates; therefore, in this study, we utilized network analysis as a principled way to quantify imagined items as nodes, and the vividness associations between the nodes as edges. With this approach, the representative structure of such an “imagination

network” captures the representational structure of the world model. Critically, the importance of different imagined nodes in the *imagination network* can be measured by different centrality measures such as expected influence, closeness, betweenness (see Methods) which quantify the utility of a node in different ways in the network. Further, the networks can be clustered into submodules utilizing community detection algorithms to estimate macroscopic properties of the network. We hypothesized that if the internal world models were similar, then the importance of imagined nodes across groups of populations would be correlated as well as show clustering alignments. Additionally, because the items in the VVIQ-2 and PSIQ questionnaires cover different contexts, we employed a cluster detection algorithm to identify clusters within each of the imagination networks, and measured the alignment of clustering between pairs of networks. We reasoned that if IWMs were similar across different experimental groups, the imagination networks should yield higher clustering alignment for our given imagination tasks.

We focused on scenarios involving reproductive imagination<sup>16</sup> related to common environmental scenarios in humans and LLM agents, as both types of agents possess the ability to generate internal representations that model the external world. Further, we interpret large language models (LLMs) as cognitive agents whose long-term memory is influenced by their architecture, training data and system message<sup>48,49</sup>. Emerging evidence suggests that even minimal sensory-style instructions (e.g., “imagine seeing...”) can guide text-only LLMs to organize their internal representations in ways that parallel modality-specific encoders. Thus, prompting may be sufficient to evoke structured, perceptual-like processing<sup>50</sup>. We treat LLMs as agents whose internal parameters encode rich statistical world knowledge acquired from text and can be utilized in our task to see inherent structural relationships among different imagination prompts using vividness ratings that can be compared to human groups’ *imagination networks*.

By administering human imagery questionnaires to both humans and LLMs, and constructing imagination networks for each, we can ask a more targeted comparative question: do humans and LLMs organize imagined scenarios according to similar dependency structures, or do their imagination networks reflect systematically different internal models of the world? Differences in these networks would be expected if human world models are grounded in multimodal experience and episodic memory, whereas LLMs' models are grounded in linguistic co-occurrence statistics.

To anticipate, our study provides evidence that imagination is employed to access internal world models, with results showing that while IWMs from different human populations were quite similar to each other, the IWMs from humans and LLMs were quite distinct. Our approach demonstrates how composite measures from network science can help us understand IWMs in both humans and LLMs using imaginative abilities. Overall, this work can facilitate future comparisons between the subjective phenomenological structures present in humans and artificial intelligence.

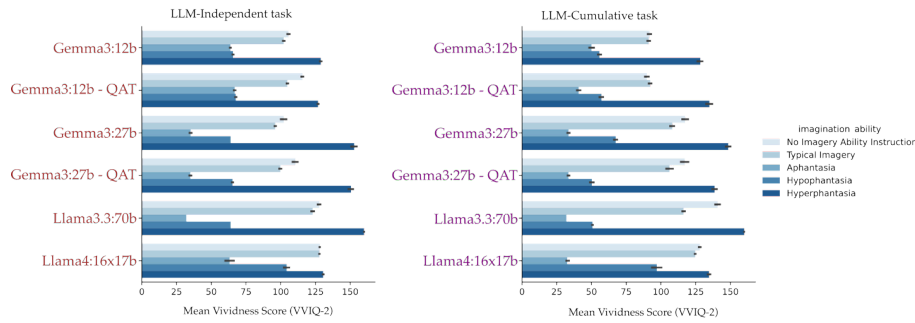
## Results

To evaluate internal world models in humans and AI, we studied responses to two imagination questionnaires (VVIQ-2 and PSIQ) from three human populations (Florida, Poland, and London) and two families of language models (Gemma and Llama). Data from Florida was collected directly by the authors for both questionnaires. Open-source data for Poland was sourced from Jankowska & Karwowski (2022)<sup>51</sup> for the VVIQ-2, while data for the PSIQ-2 from London was sourced from Clark & Maguire (2023)<sup>52</sup>. We utilized different human population groups and imagination tasks to elucidate the generalization of our results using network analysis. Each questionnaire focuses on various scenarios and contexts: the VVIQ-2 asks

participants to imagine eight different environmental scenes, while the PSIQ asks participants to imagine sensory experiences in seven different modalities, including emotional experiences. We constructed imagination networks separately from (1) vividness ratings from human datasets, and (2) vividness ratings from LLM responses. On the VVIQ-2, humans and LLMs reported vividness on a scale of 1 to 5; for the PSIQ, vividness was rated on a scale of 0 to 10 for each item.

We compared network measures across humans and LLMs using two approaches: an “LLM-Independent task” where LLMs rated items separately, and an “LLM-Cumulative task” where they used previous conversation history. This created 12 unique artificial population groups from the Gemma and Llama family models, which vary in size and training. We also compared different LLM populations with each other to evaluate similarity across IWMs from LLM agents for the network analysis. We observed that LLMs could report vividness ratings, which varied based on instructions regarding imagination ability (see Methods). LLM agents demonstrated diverse imagination abilities, as indicated by total vividness scores (Fig. 1A).

A. LLM’s mean vividness across imagination ability.



B. Mean (left) and distribution (right) of total vividness score in Humans and after population diversity sampling in LLMs.

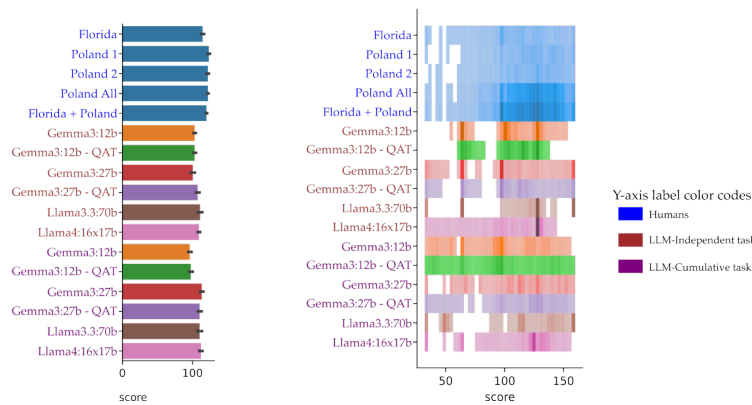


**Fig 1. Total VVIQ-2 vividness scores and distributions in LLMs and human populations.** (A) Mean vividness scores across different VVIQ-2 LLM simulations. The total score is the sum of all vividness ratings in the questionnaire. For each LLM in a task (independent or cumulative), 1000 simulations were performed using 200 personalities and five imagination ability conditions. (B) (Left) Average total vividness scores from human populations and each LLM agent after population diversity sampling (to increase variability in the imagination abilities of LLMs; see Methods), with 600 simulations from different imagination abilities. (Right) Distributions of the total vividness scores in humans and LLM agents for the VVIQ-2. Darker colors denote a higher density of data in that bin for a given population of cognitive agents (human or LLM). See Fig. S1 for vividness scores for the PSIQ. The error bars in bar plots are bootstrapped ( $N = 1000$ ) 95% confidence intervals.

To investigate how prompting and LLM task conditions influenced overall vividness ratings, we used the Kruskal-Wallis test to analyze the aggregate effect on total vividness scores, which were the sum of all vividness ratings across the imagined items from the VVIQ-2 or PSIQ (LLM results reflect 1000 total simulations based on 200 personalities and five imagination abilities; see Methods). For the VVIQ-2, the minimum score is 32, and the maximum score is 160. We found a significant main effect of imagination ability prompts ( $H(4) = 9588.31, p < 0.0000001$ ); LLM-task: independent or cumulative ( $H(1) = 49.194, p = 2.319 \times 10^{-12}$ ) and model ( $H(5) = 460.8, p = 2.297 \times 10^{-97}$ ). Using Dunn’s post-hoc comparisons, we found that all

pair-wise comparisons for different levels of imagination ability (no imagery, typical imagery, aphantasia, hypophantasia, hyperphantasia) prompts given to LLMs showed significant differences. The increase in total vividness score was found to increase with improved imagination ability, from aphantasia (lowest total vividness score, marginal mean = 43.2) to hyperphantasia (highest total vividness score, marginal mean = 141.3). Surprisingly, intermediate levels of the “no imagination ability” condition (marginal mean = 114.6) had a higher total vividness score compared to the “typical imagery” ability (marginal mean = 107.8).

We found that the LLM-cumulative task, on average, had a higher total vividness score than the LLM-independent task ( $z = -7.014$ ,  $p_{holm} < 0.000001$ ) with marginal means of 97.35 and 92.33, respectively. For the LLM agents, all models had total vividness scores that were significantly different from each other, and we found that the total vividness score was lowest for Gemma3:12b (marginal mean = 88.34) and highest for Llama4:16x17b (marginal mean = 107.101), indicating a trend of increasing total vividness ratings from the smallest to the largest model, suggesting the LLM models are inherently different in how they report vividness ratings. Together, these results show that our manipulations of LLM-task (independent or cumulative) and imagination ability prompts led to significant behavioral changes in vividness reports from each LLM utilized in our study. We found similar patterns of results for the PSIQ data (Supplementary Fig. S1A).

As human populations consist of individuals with varying imagination abilities, we aimed to introduce variability in the imagination ability of the LLM agents’ population by performing population diversity sampling (see Methods). The total vividness scores for LLMs after population diversity sampling, along with experimental human data groups in VVIQ-2, are illustrated in Fig. 1B. (corresponding figures for the PSIQ are plotted in Supplementary Fig. 1B).

Since the total vividness score is not parametrically distributed (Fig. 1B (right)), we performed a pair-wise Kolmogorov-Smirnov (K-S) test with Benjamini/Hochberg FDR correction for multiple comparisons, as we did not have an *a priori* hypothesis for these comparisons. We found that the distribution for total vividness scores for the *Florida + Poland* group was significantly different from the *Florida* ( $statistic = 0.07, p_{BH} = 0.035$ ) and *Poland* groups ( $statistic = 0.11, p_{BH} < 0.001$ ), whereas all other comparisons of human groups with each other in VVIQ-2 did not show a significant difference. The pairwise comparisons of LLM groups in Fig. 1B among themselves and with human groups were significantly different from each other. The univariate analysis of total vividness ratings reveals that the population of different cognitive agents (natural or artificial) exhibits varying amounts of vividness in their overall imaginative experiences; however, this analysis does not provide insights regarding relationships about the importance of one imagined scenario to another scenario.

### Overview of Network Estimation

Our conceptualization of imagination is that the vividness of an imagined scenario depends on its importance in relation to other imagined scenarios, and that importance depends on long-term memories of cognitive agents. Evaluating the relationships between imagination scenarios necessitates multivariate analysis; in this work, we utilized tools from network science, and visualized our results as imagination networks (see Fig. 2 for the VVIQ-2, and Fig. 3 for the PSIQ). Our analysis of different human populations facilitated comparisons both within and across geographic regions for the VVIQ-2. For example, in our study of human responses to the VVIQ-2, we constructed networks for one population from *Florida* ( $N = 541$ ), two different populations from Poland: *Poland 1* ( $N = 600$ ) and *Poland 2* ( $N = 600$ ), a combination of the two Polish populations (*Polish All*,  $N = 1651$ ), and a combined *Florida + Polish* ( $N = 2192$ )

population. For the PSIQ imagination networks, we utilized data from *Florida* ( $N=334$ ), *London* ( $N=217$ ), and *Florida+London* ( $N=551$ ). We reasoned that if the IWMs differed across composite groups from the VVIQ-2 (*Poland All*, *Florida+Poland*) and PSIQ (*Florida+London*), then the correlation patterns of node importance (via centrality measures) would shift in the opposite direction when compared to non-overlapping groups (Florida, Poland 1, Poland 2, and London) in the respective imagination tasks (VVIQ-2 or PSIQ).

Furthermore, we synthesized different populations of vividness reports from LLM agents with stateful (LLM-Cumulative) and stateless (LLM-Independent) LLM tasks based on human imagination abilities (see Methods) using models from Gemma3, Llama3.3, and a Mixture of Experts (MoE) Llama4:16x17b. We measured the correlations between centrality measures and clustering alignments across imagination networks to capture the similarity between specific pairs of internal world models. That is, since our measurements of the internal world rely on the similarity of network properties, including the correlation of centralities (the importance of an imagined node) and clustering alignments of imagination networks, we can infer whether two given cognitive agent populations had a high degree of similarity in their IWMs.

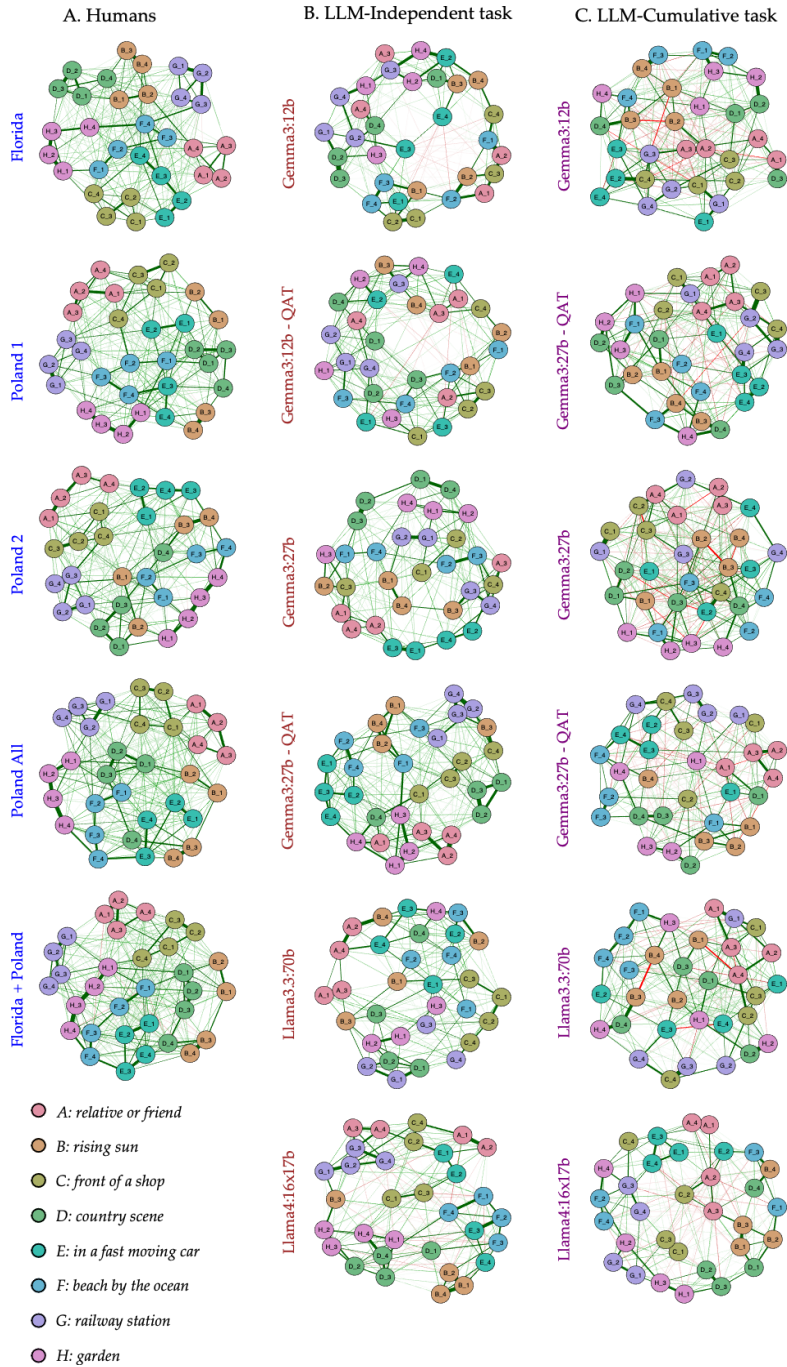


**Fig. 2. Imagination networks using the VVIQ-2 in Humans and LLMs.** Cognitive agents (humans or LLMs) report the vividness of imagined items across different contexts of the environment, denoted as different colors in the networks. There are four items in each context, with postfixed numerals labeling each node. The vividness rating is reported on a scale of 1 to 5. The network was estimated using the EbicGlasso method using Spearman partial correlations of vividness ratings between different pairs of nodes. (A) Imagination networks in human populations: Florida ( $N = 541$ ), Poland-1 ( $N = 600$ ), Poland-2 ( $N = 600$ ), Poland-All ( $N = 1651$ ), Florida+Poland ( $N = 2192$ ), from top to bottom. (B) LLM imagination networks from Gemma and Llama variants in independent task conditions. (C) In the LLM imagination networks in the cumulative task condition, each scene’s vividness rating is provided utilizing the conversation history of previous interactions (i.e., previous responses to items on the questionnaire). Each LLM network consists of  $N = 600$  simulations. The color and thickness of an edge indicates its magnitude and direction of association. Red lines indicate negative associations and green lines indicate positive associations for an edge.

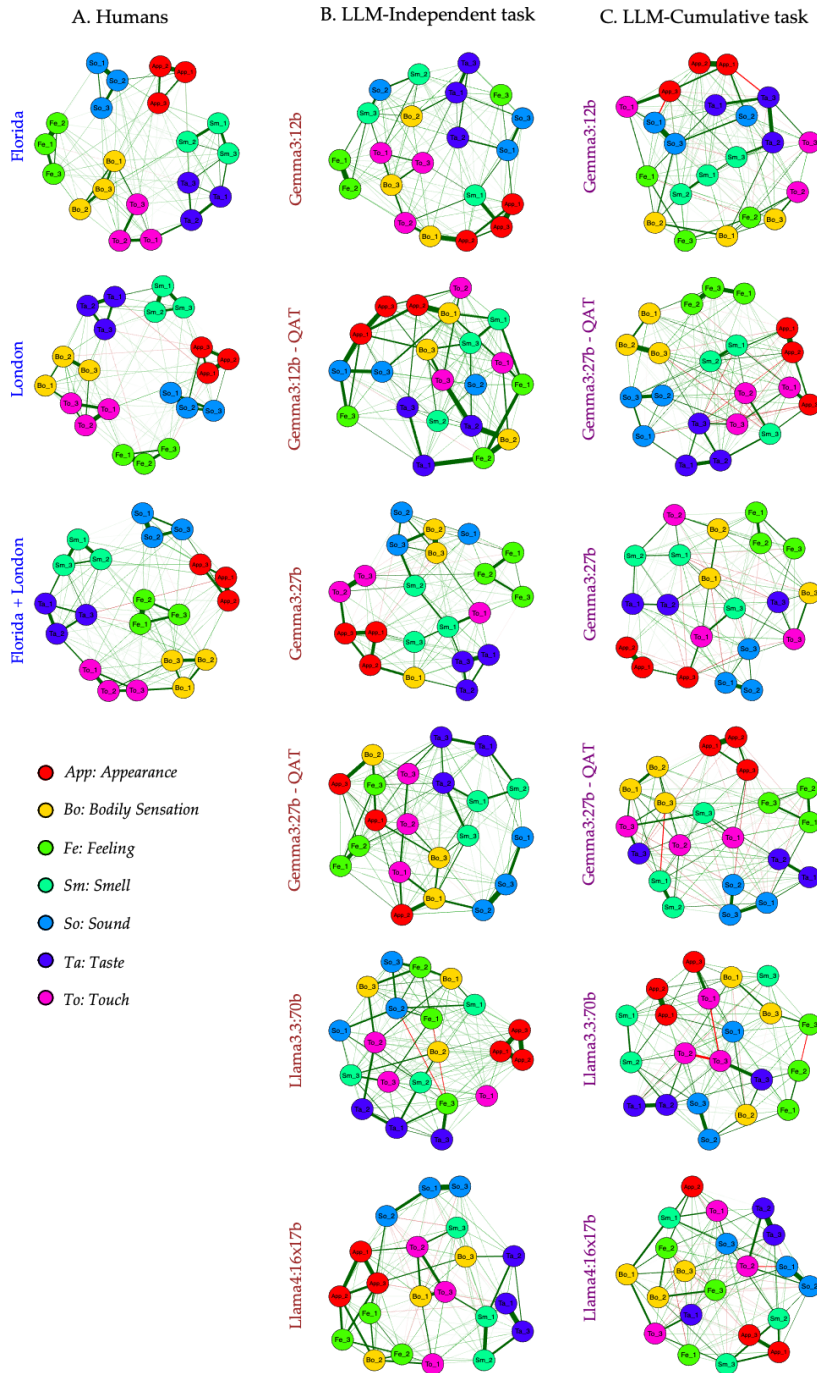


**Fig. 3. Imagination networks using the PSIQ in Humans and LLMs.** Cognitive agents (humans or LLMs) report the vividness of imagined items across different contexts of sensory experiences, denoted as different colors in the networks. There are three items in each context, with postfixed numerals to each node. The vividness rating is reported on a scale of 0 to 10. The network is estimated using the EbicGlasso method using Spearman partial correlations of vividness ratings between different pairs of nodes. (A) Imagination networks in human populations: Florida (N = 334), London (N = 217), and Florida+London (N = 551), from top to bottom. (B) LLM imagination networks in the independent task condition. Each node’s vividness rating is rated independently. (C) In the LLM imagination networks in the cumulative task condition, each item’s vividness rating is rated with the conversation history of previous interactions. Each LLM network consists of N = 600 simulations. The color of nodes signifies the modality in the PSIQ, with three items in each modality. The color and thickness of an edge indicate its magnitude and direction of association. Red lines indicate negative associations and green lines indicate positive associations for an edge.

In both human and LLM networks, each node represents a questionnaire item that was imagined, and edges between nodes capture the degree of associations between vividness ratings. To compute the graphical model, we used the EBICglasso with the Spearman correlation method. The EBICglasso method penalizes partial correlations to reduce false-positive edges (see Methods for details). For each node in the network, we calculated four centrality measures: (i) expected influence, (ii) strength, (iii) closeness, and (iv) betweenness. The four centrality measures characterize the importance of a node in a network in different ways, in terms of its relationships with other nodes, and in relation to information processing. Expected influence and strength capture the influence of a node over the network due to its direct connections with other nodes in the imagination network. Specifically, expected influence is the summation of signed edges to a node, and strength is the summation of unsigned edges at the nodes. Thus, expected influence and strength are local measures that only account for direct connections with other nodes and reveal how a node influences the overall network topology due to its associations with other nodes in a network. In contrast, closeness and betweenness are measures of global centralities, which account for direct and indirect connections between nodes in a given network. Specifically, closeness measures how information can flow to other nodes by calculating the shortest distance to each node in the network, and betweenness measures the frequency at which a node appears in the shortest paths between pairs of nodes in a given network. Therefore, closeness and betweenness measure the importance of a node in terms of how information can travel in a network to other nodes, either directly or indirectly connected with a given node.

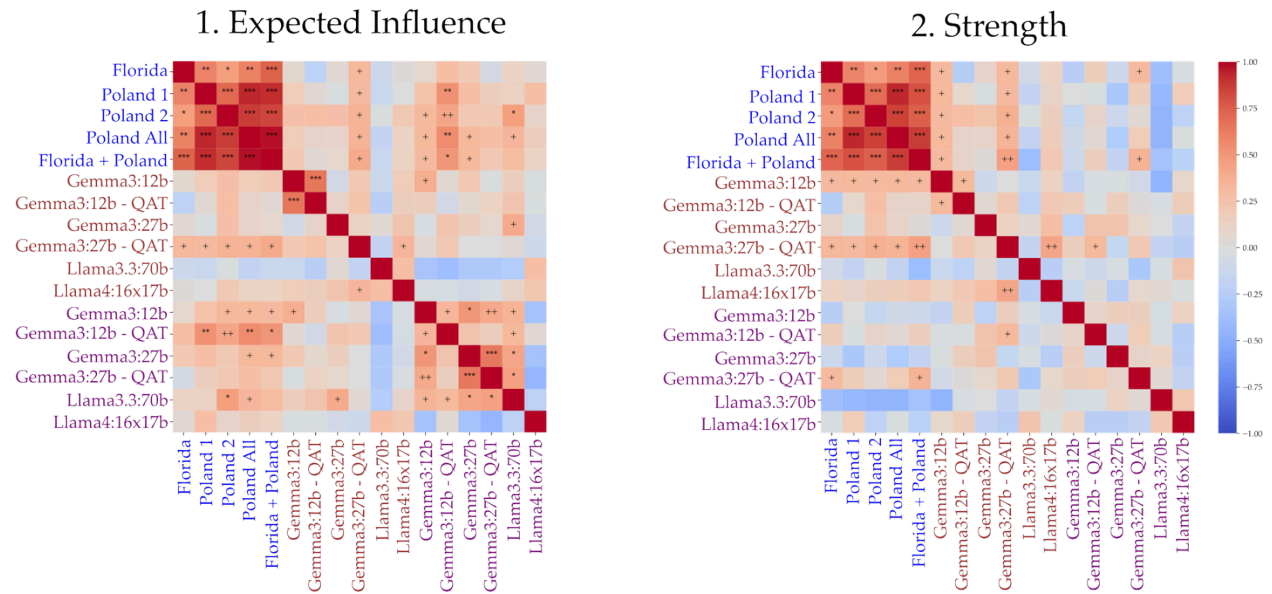
These centrality measures allow us to evaluate the structure of imagination networks in humans and LLMs at a micro-topological level. If human IWMs are structurally similar across populations, these four measures should show a positive degree of correlation across different

human networks. Further, we examined whether the nodes were similarly clustered across different imagination networks by computing the pairwise Adjusted Rand Index, or ARI<sup>53</sup>, which measures the degree of agreement in node assignments across clusters between two networks. This measure accounts for chance-level similarity rates between nodes within the same clusters across networks, thereby characterizing the meso-level topological features of an internal world model using imagination networks. Networks having a higher ARI score signify that the internal world model is similarly clustered across two given imagination networks.

**Expected influence and strength reveal high correlations within human populations, highlighting the importance of nodes in imagination networks.**

We found consistently high correlations among local centrality (expected influence and strength) measures in human populations in each of the imagination networks (VVIQ-2 or PSIQ), suggesting that human populations have correlated internal world models during imagination (Fig. 4). Further, the correlations of centrality increased when the homogenous population groups (Florida, Poland-1, Poland-2, or London) were compared to composite groups (e.g. Florida versus Poland All or Florida+Poland, Poland 1 versus Poland All in VVIQ; Florida versus Florida+London). Whenever there was a violation of bivariate normality, as indicated by the Shapiro-Wilk test, we reported Spearman's rho as the correlation coefficient in all pairwise centrality correlations, although in Fig. 4, we only illustrate Pearson's r correlations.

A. VVIQ-2 Local Centrality Correlations



B. PSIQ Local Centrality Correlations

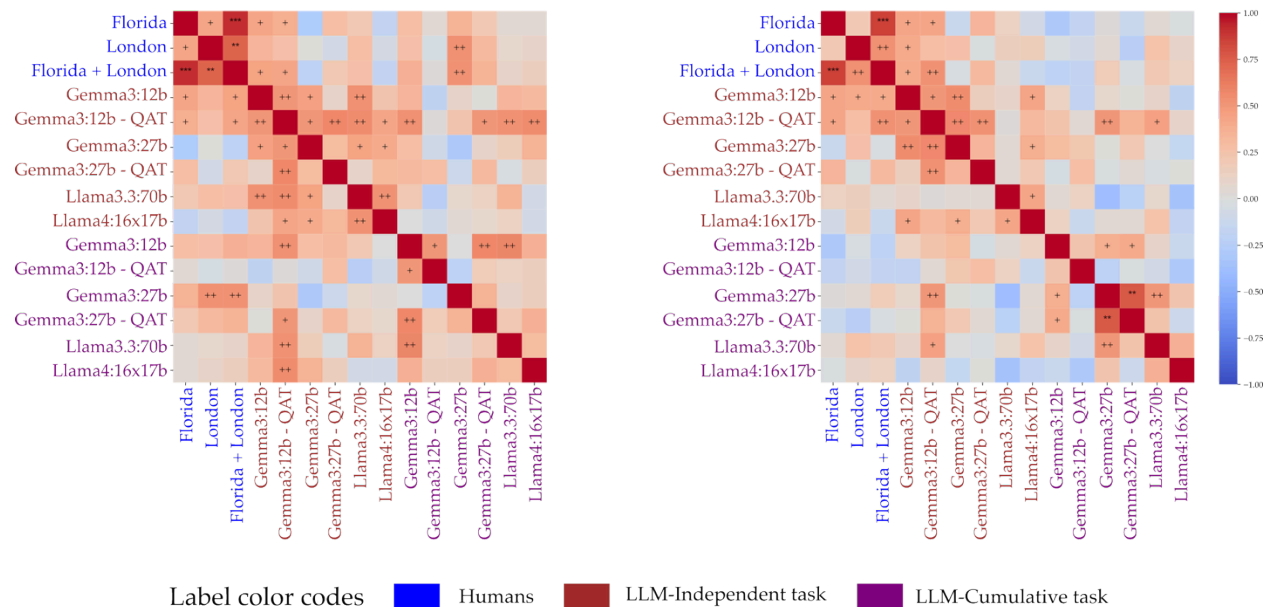


**Fig. 4. Pearson’s r correlation heatmaps of node importance using different local centrality measures across VVIQ-2 and PSIQ imagination networks.** The left column denotes correlations for expected influence; the right column denotes correlations for strength. (A) Centrality correlations among cognitive agents for the nodes in VVIQ-2 imagination networks with 32 nodes (*top row*). (B) Centrality correlations among cognitive agents for the nodes in PSIQ imagination networks with 21 nodes (*bottom row*). Expected influence and strength centralities exhibited high correlations among human populations for the VVIQ-2, and a similar pattern of results was found for the PSIQ. + denotes a significant result based on uncorrected p-values and \* denotes significant result based on corrected p-values using Benjamini/Hochberg FDR correction for multiple comparisons; \*/+ < 0.05; \*\*/+ < 0.01; \*\*\* < 0.001. The heatmaps are symmetric across the top-left to bottom-right diagonal.

For VVIQ-2 imagination networks with 32 nodes, positive correlations for expected influence centrality were exhibited among human networks (Fig. 4A-1) (*Florida vs Poland 1*:  $r = 0.589$ ,  $p = 0.000195$ ,  $p_{BH} = 0.002413$ ; *Florida vs Poland 2*:  $r = 0.466$ ,  $p = 0.0036$ ,  $p_{BH} = 0.03$ ; *Florida vs Poland All*:  $r = 0.595$ ,  $p = 0.000163$ ,  $p_{BH} = 0.002$ ; *Florida vs Florida+Poland All*:  $r = 0.732$ ,  $p = 0.000001$ ,  $p_{BH} = 0.000022$ ; *Poland 1 vs Poland 2*:  $r = 0.712$ ,  $p = 0.000002$ ,  $p_{BH} = 0.000048$ ; *Poland 1 vs Poland All*:  $r = 0.931$ ,  $p < 0.000001$ ,  $p_{BH} < 0.000001$ ; *Poland 1 vs Florida+Poland All*:  $r = 0.92$ ,  $p < 0.000001$ ,  $p_{BH} < 0.000001$ ; *Poland 2 vs Poland All*:  $r = 0.86$ ,  $p < 0.000001$ ,  $p_{BH} < 0.000001$ ; *Poland 2 vs Florida+Poland All*:  $r = 0.837$ ,  $p < 0.000001$ ,  $p_{BH} < 0.000001$ ; *Poland All vs Florida+Poland*:  $p < 0.000001$ ,  $p_{BH} < 0.000001$ ). In the sensory imagination networks using the PSIQ with 21 nodes as shown in Fig. 4B-1, we again found similar patterns of correlation values across human networks in expected influence (*Florida vs London*:  $r = 0.425$ ,  $p = 0.027$ ,  $p_{BH} = 0.12$ ; *Florida vs Florida+London*:  $r = 0.914$ ,  $p < 0.000001$ ,  $p_{BH} < 0.000001$ ;  $\rho = 0.848$ ,  $p < 0.000001$ ,  $p_{BH} < 0.000001$ ; *London vs Florida+London*:  $r = 0.733$ ,  $p = 0.000079$ ;  $\rho = 0.622$ ,  $p = 0.001302$ ,  $p_{BH} = 0.034$ ).

For the VVIQ-2 tasks, the correlations with LLM models in different tasks (independent and cumulative) were inconsistent; only Gemma3:27b-QAT in the independent task showed weakly significant correlations, ranging from 0.308 ( $p = 0.04$ ,  $p_{BH} = 0.159293$ ) with *Poland 1* to 0.393 ( $p = 0.013$ ,  $p_{BH} = 0.078730$ ) with *Florida+Poland*. Other models in LLM cumulative tasks, such as Gemma3:12b, Gemma3:12b-QAT, Gemma3:27b, and Llama3.3:70b showed increased and significant correlations of expected influence, ranging from  $r = 0.3$  ( $p = 0.043$ ,  $p_{BH} = 0.16$ ; Gemma3:12b with *Florida+Poland*) to  $r = 0.548$  ( $p = 0.000582$ ,  $p_{BH} = 0.0066$ ; Gemma3:12b-QAT with *Poland All*).

For the PSIQ and LLM-independent task data, only Gemma3:12b and Gemma3:12b-QAT correlated with Florida ( $r = 0.432, p = 0.025, p_{BH} = 0.12$ ;  $r = 0.38, p = 0.041, p_{BH} = 0.16$ , respectively) and Florida+London groups ( $r = 0.44, p = 0.022, p_{BH} = 0.11$ ;  $r = 0.435, p = 0.024, p_{BH} = 0.11$ , respectively). During the LLM-cumulative task, these models were not found to be significantly correlated with the human models. Similarly, the remaining LLM models were also not significantly correlated with the human groups. Still, we found the Gemma3:27b in the cumulative task to show correlation with Florida+London ( $r = 0.52, p = 0.0078, p_{BH} = 0.06$ ) and London ( $r = 0.52, p = 0.007, p_{BH} = 0.06$ ) imagination networks.

Strength centrality showed significant correlations in human groups for VVIQ-2 imagination networks (Fig. 4A-2) (*Florida vs Poland 1*:  $r = 0.591, p = 0.000184, p_{BH} = 0.002788$ ; *Florida vs Poland 2*:  $r = 0.479, p = 0.002766, p_{BH} = 0.037621$ ; *Florida vs Poland All*:  $r = 0.596, p = 0.000159, p_{BH} = 0.002710$ ; *Florida vs Florida+Poland All*:  $r = 0.725, p = 0.000001, p_{BH} = 0.000031$ ; *Poland 1 vs Poland 2*:  $r = 0.692, p = 0.000006, p_{BH} = 0.000114$ ; *Poland 1 vs Poland All*:  $r = 0.928, p < 0.000001, p_{BH} < 0.000001$ ; *Poland 1 vs Florida+Poland All*:  $r = 0.797, p < 0.000001, p_{BH} = 0.000001$ ; *Poland 2 vs Poland All*:  $r = 0.85, p < 0.000001, p_{BH} < 0.000001$ ; *Poland 2 vs Florida+Poland All*:  $r = 0.749, p < 0.000001, p_{BH} = 0.000011$ ; *Poland All vs Florida+Poland All*:  $r = 0.86, p < 0.000001, p_{BH} < 0.000001$ ). Regarding LLM responses for the VVIQ-2, for the LLM Independent Task, Gemma3:12 showed significant correlations for strength in the range of 0.302 to 0.326 with all human populations. Similarly, Gemma3:27-QAT exhibited significant correlations with all human populations, ranging from 0.305 to 0.452. In the LLM-cumulative task, only Gemma3:27-QAT showed significant correlations with the Florida ( $r = 0.304, p = 0.045$ ) and Florida+Poland ( $r = 0.357, p = 0.022$ ) groups; most correlations failed to be significant after multiple corrections.

For imagination networks based on the PSIQ, we found a similar pattern of results for the strength centrality (Fig. 4B-2), too, which was significantly correlated with composite human groups (*Florida vs Florida+London*:  $r = 0.858$ ,  $p < 0.0000001$ ,  $p_{BH} = 0.000035$ ; *London vs Florida+London*:  $r = 0.538$ ,  $p = 0.006$ ,  $p_{BH} = 0.11$ ). Regarding LLM responses, in the LLM independent task, strength measures from Gemma3:12 were found to be significantly correlated with all the human groups (*Florida*:  $r = 0.422$ ,  $p = 0.028$ , *London*:  $r = 0.413$ ,  $p = 0.031$ , *Florida+London*:  $r = 0.404$ ,  $p = 0.035$ ); Gemma3:12-QAT was correlated with *Florida* ( $r = 0.429$ ,  $p = 0.026$ ) and *Florida+London* ( $r = 0.518$ ,  $p = 0.008$ ) group in the independent task, but these models did not show significant correlations in cumulative task. Overall, all other strength measures from LLM's in either task (independent or cumulative) were found to be not significant; often, these correlations were insignificant after corrections to *p-values* for multiple comparisons. Thus, based on our evidence of measuring local centrality measures of expected influence and strength correlations as the measure of importance of imagined nodes in the internal world model during VVIQ-2 (eight environmental contexts with 32 items in total) and PSIQ (seven sensory contexts with 21 items in total), human networks are highly similar.

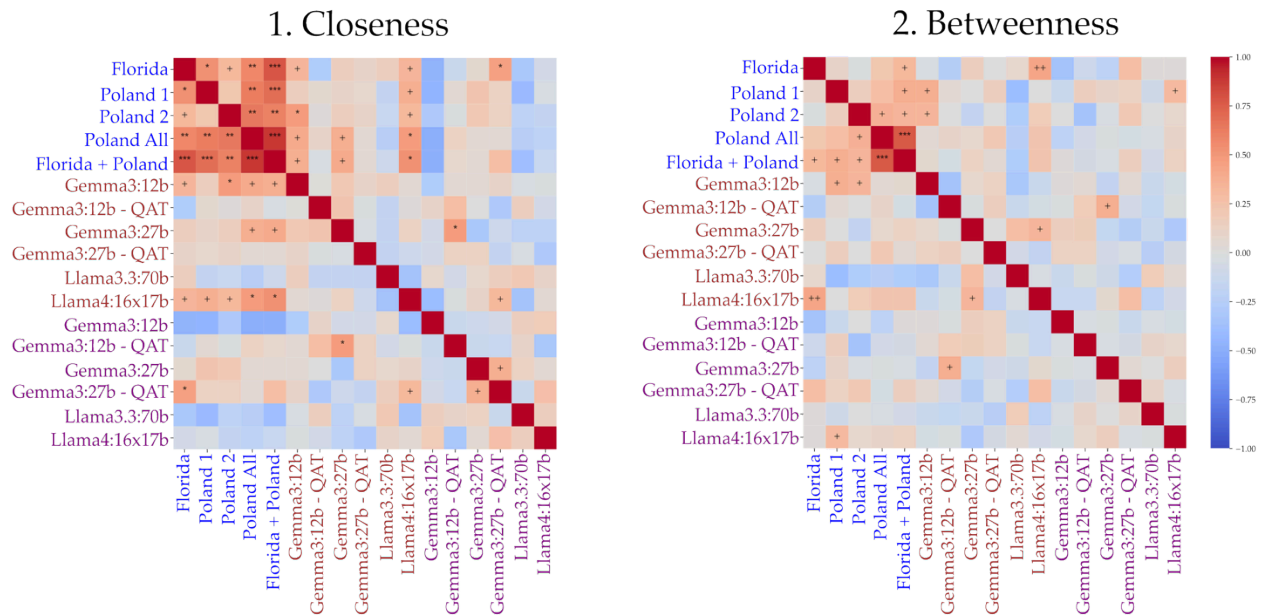
**In humans, imagined nodes are highly correlated for closeness, but not for betweenness.**

Closeness measures how information can flow to other nodes by calculating the shortest distance to each node in the network. The higher the closeness of a node, the more it is involved in the imagination of the other nodes in the imagination network. Human imagination networks based on the VVIQ-2 revealed highly significant correlations for closeness measures (Fig. 5, left column) (*Florida vs Poland 1*:  $r = 0.535$ ,  $p = 0.000795$ ,  $p_{BH} = 0.0136$ ; *Florida vs Poland 2*:  $r = 0.313$ ,  $p = 0.041$ ,  $p_{BH} = 0.23$ ; *Florida vs Poland All*:  $r = 0.572$ ,  $p = 0.000311$ ,  $p_{BH} = 0.006045$  ( $\rho = 0.48$ ,  $p = 0.0025$ ,  $p_{BH} = 0.034$ ); *Florida vs Florida+Poland All*:  $r = 0.776$ ,  $p < 0.000001$ ,

$p_{BH} = 0.000006$ ; *Poland 1 vs Poland All*:  $r = 0.619$ ,  $p = 0.00008$ ,  $p_{BH} = 0.002$  ( $\rho = 0.62$ ,  $p = 0.000075$ ,  $p_{BH} = 0.0025$ ); *Poland 1 vs Florida+Poland All*:  $r = 0.684$ ,  $p = 0.000008$ ,  $p_{BH} = 0.000365$ ; *Poland 2 vs Poland All*:  $r = 0.64$ ,  $p = 0.00004$ ,  $p_{BH} = 0.001$  ( $\rho = 0.43$ ,  $p = 0.0072$ ,  $p_{BH} = 0.088$ ); *Poland 2 vs Florida+Poland All*:  $r = 0.604$ ,  $p = 0.000126$ ,  $p_{BH} = 0.002849$ ; *Poland All vs Florida+Poland All*:  $r = 0.884$ ,  $p < 0.000001$ ,  $p_{BH} < 0.000001$  ( $\rho = 0.86$ ,  $p < 0.000001$ ,  $p_{BH} < 0.000001$ ). With PSIQ imagination networks, we found similar patterns (Florida vs London:  $r = 0.759$ ,  $p = 0.000033$ ,  $p_{BH} = 0.001147$ ; Florida vs Florida+London:  $r = 0.874$ ,  $p < 0.000001$ ,  $p_{BH} = 0.000012$ ; London vs Florida+London:  $r = 0.842$ ,  $p = 0.000001$ ,  $p_{BH} = 0.000044$ ).

While examining the LLMs, as in the local (expected influence and strength) centralities, we found no consistent pattern of correlations with the human groups, and they rarely survived corrections for multiple comparisons in both the imagination tasks. An interesting pattern, however, emerged for correlations of closeness centrality across VVIQ-2 and PSIQ, with more LLMs across LLM-tasks (independent or cumulative) showing higher correlations for PSIQ scores with humans, suggesting a task-dependent nature of centrality correlation across humans and LLMs (Fig. 5-A1 and B1).

A. VVIQ-2 Global Centrality Correlations



B. PSIQ Global Centrality Correlations

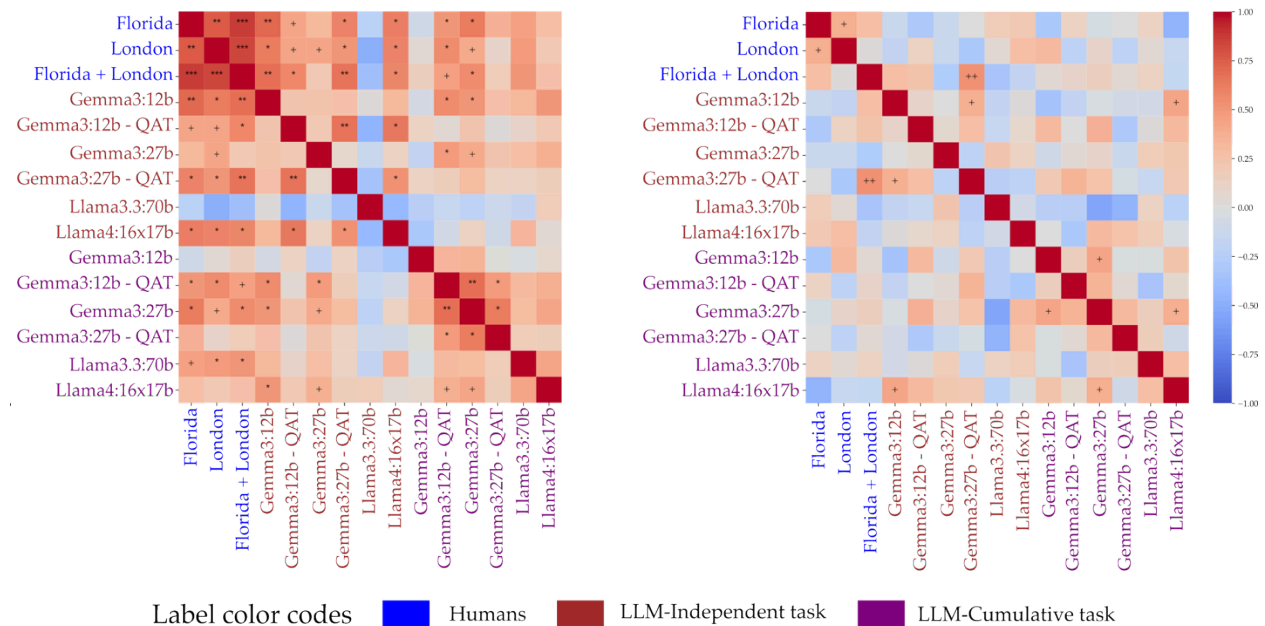


**Fig. 5. Pearson’s r correlation heatmaps of node importance using different global centrality measures across VVIQ-2 and PSIQ imagination networks.** Columns, left to right, display different centrality measures; specifically, closeness and betweenness. (A) Centrality correlations among cognitive agents for the nodes in VVIQ-2 imagination networks with 32 nodes (*top row*). (B) Centrality correlations among humans but not in betweenness for the nodes in PSIQ imagination networks with 21 nodes (*bottom row*). Closeness centrality correlations across cognitive agents show high correlations among human populations across VVIQ-2 and PSIQ. Betweenness centrality results show a lack of centrality correlations across cognitive agents in both VVIQ-2 and PSIQ. + denotes significance based on uncorrected p-values and \* denotes significance based on corrected p-values using Benjamini/Hochberg FDR correction for multiple comparisons; \*/+ < 0.05; \*\*/++ < 0.01; \*\*\* < 0.001. The heatmaps are symmetric across the top-left to bottom-right diagonal.

Among all the centralities, the correlations for betweenness centrality across cognitive agents (humans and LLMs) showed the weakest correlations (Fig. 5-A2 and B2), suggesting the possibility of individual differences in how important an imagined node is in terms of its being frequented between two nodes. Further, among all the centrality measures we estimated, betweenness showed the least stability, at times displaying values below 0.25 in terms of the CS-Coefficient<sup>54</sup> (Table-S1 and Table-S2). The CS-coefficients were evaluated by calculating centralities in subsamples of the data, and the lack of stability for betweenness centrality again suggests that it exhibits high individual differences in how an imagined node is utilized in relation to other pairs of imagined nodes.

Finally, among all four centrality measures, expected influence, strength, and closeness lead us to conclude that imagination networks were similar across human populations, suggesting a general property of IWMs. In contrast, betweenness suggests that the IWMs will still exhibit individual differences in terms of the frequency with which an imagined node is present in the imagination network between two nodes.

**Clustering is prominent in human networks, and often absent in LLM agents for imagination networks.**

Data-based clusters were computed from the imagination networks (Fig. 2 and Fig. 3) and calculated using the walk-trap algorithm<sup>55,56</sup> to measure the meso-level properties of the imagination networks. As centralities capture the micro-level properties of the network at the node level, one can investigate the meso-characteristics of the network in terms of how a group of nodes cluster together<sup>57,58</sup>. The walk-trap algorithm is a community detection algorithm that identifies communities/clusters of nodes characterized by dense connections among themselves, rather than to other nodes in the network. As the VVIQ-2 and PSIQ require imagination of

diverse scenarios representing specific contexts, we asked the following question: do nodes of imagination networks from human and LLM cognitive agents exhibit clustering? We analyzed data from the VVIQ-2, and found that while human imagination networks exhibited characteristic clustering patterns that reflected the different scenes used in the questionnaire, LLM-based imagination depended on the model and LLM task (independent or cumulative). As shown in Supplemental Table S3, the imagination networks from the VVIQ-2 human data could be decomposed into six clusters for *Florida*, five clusters for *Poland 1*, six clusters for *Poland 2*, four clusters for *Poland All*, and five clusters for *Florida+Poland* groups. In the LLM independent task for VVIQ-2, the imagination network could be decomposed into only one cluster for Gemma3:12b, Gemma3:12b-QAT, Gemma3:27b, Gemma3:27b-QAT, Llama3.3-70b, while the MoE (mixture-of-expert) model Llama4:16x17b had three clusters. In the LLM cumulative task, Gemma3:12b-QAT and Llama3.3:70b still consisted of a single cluster, whereas Gemma3:12b increased to four clusters, Gemma3:27b increased to four clusters, Gemma3:27b-QAT increased to five clusters, and MoE Llama4:16x17b increased to four clusters. Together, these results suggest that the model type/size and presence of conversation memory (as in the cumulative task) have differential effects on the clustering of the imagination network based on VVIQ-2.

As shown in Supplemental Table S4, for the PSIQ-based imagination networks, human groups again showed clustering, with five clusters in *Florida*, four clusters in *London*, and five clusters in *Florida+London*. In the LLM independent task, all LLM models had only a single cluster, whereas in the LLM cumulative task, all models had single clusters, except for Gemma3:27b-QAT, which had five clusters. Overall, human population groups showed consistent clustering in different types of imagination networks (VVIQ-2 or PSIQ), whereas the

clustering in imagination networks formed using responses from LLMs depended on the model, task type (independent or cumulative), and type of imagination task (VVIQ-2 or PSIQ).

As VVIQ-2 and PSIQ results both indicate the presence of data-based clustering in the imagination networks, we utilized the adjusted rand index (ARI), which accounts for chance-level alignment of clusters across two clustering groups, to quantify the degree of clustering alignment between the two networks. An ARI closer to 1 reflects high alignment between the clustering. At the same time, a negative ARI indicates that the clustering is worse than random, and an ARI of 0 demonstrates that the clustering alignment is no better than random.

In general, human imagination networks from VVIQ-2 data showed more clustering alignment than the relationships between LLM networks and human networks. As shown in Fig. 6A, for VVIQ-2 imagination, the *Florida* group had an ARI of 0.29 with *Poland 1*, 0.40 with *Poland 2*, 0.27 with *Poland All*, and 0.39 with *Florida+Poland*. In the LLM independent task, most LLMs exhibited only one cluster and had an ARI of 0 with human groups but an ARI of 1 among themselves. The specific values are given in Supplemental table S5. Out of all models we tested, only the mixture-of-experts Llama4:16x17b showed clustering with more than one cluster. However, Llama4:16x17b's clustering alignment with the human imagination networks was lower than that of human groups among themselves, with the highest ARI being 0.22 with the *Florida+Poland* group in the LLM independent task. On the other hand, the same model in the LLM cumulative task showed a reduction in ARI with human groups, with the highest ARI being 0.20 with the *Florida* group. Although some models showed an increase in the LLM cumulative task, like Gemma3:12b (max ARI of 0.24 with *Poland All*), Gemma3:27b (max ARI of 0.3 with *Poland 2*), Gemma3:27b-QAT (max ARI of 0.17 with *Poland All*), the

Llama4:16x17b (max ARI of 0.2 with *Florida* group) had the highest clustering alignment with human VVIQ-2 imagination networks.

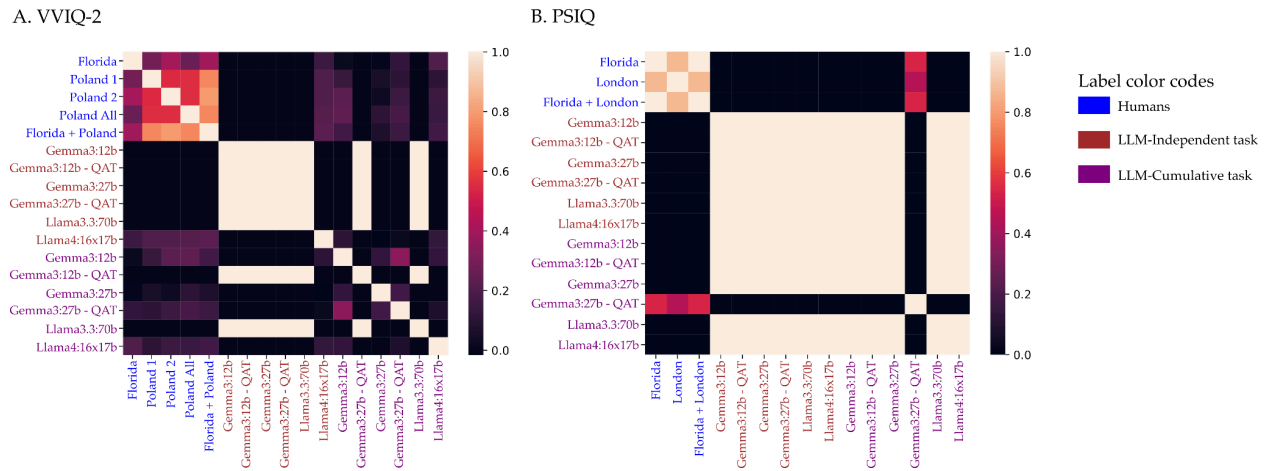


**Fig. 6. Alignment of clusters across imagination networks, as measured using the Adjusted Rand Index.** (A) Clustering alignment in the imagination network from the VVIQ-2 task. (B) Clustering alignment in the imagination network from the PSIQ task. The heatmap matrices are symmetric, from the top-left to the bottom-right diagonal.

Similarly, as shown in Fig. 6B, imagination networks from the PSIQ data also showed more clustering alignment within human groups, compared to clustering alignment between LLMs and human groups. The specific values are given in Supplemental table S6. The PSIQ imagination network of the *Florida* group exhibited an ARI of 0.87 with the *London* group and an ARI of 1 with the *Florida+London* group, while the *London* group had an ARI of 0.87 with the *Florida+London* group. All the LLMs in the independent task had an ARI of 0 with human groups, as the LLMs had only one cluster. In the cumulative task, only Gemma3:27b-QAT showed clustering as discussed above, with its ARI being 0.54 with the *Florida* group, 0.45 with the *London* group, and 0.54 with the *Florida+London* group. However, these ARIs were lower than the ARIs obtained for all within-human group comparisons. LLMs with only one cluster had a high ARI of 1 with each other. Overall, our clustering alignment results suggest that the human groups have consistently higher clustering alignment with each other across imagination

tasks, and that LLMs fail to exhibit similar clusters to those of human imagination networks, often resulting in a single cluster. Finally, in human imagination networks, the amount of clustering alignment can depend on the type of imagination task, as the PSIQ showed a higher ARI than the VVIQ-2 imagination networks.

### Discussion

Using network analysis, we provide a novel demonstration of how imagination about different scenes and sensations, as reflected in the VVIQ-2 and PSIQ, can be utilized to investigate internal world models in humans and large language models. Our findings indicate that humans organize their internal world models differently from LLMs, as demonstrated by the use of vividness ratings in response to imagination prompts across different scenes. Specifically, our clustering analysis revealed that human population-level imagination networks are often clustered compared to those of LLMs, and the degree of clustering alignment in human populations varies depending on the type of imagination task. Our imagination networks estimated using EBICglasso and Spearman pairwise partial correlations<sup>54</sup> highlight the correlated importance of nodes (imagined scenes) within human networks and also show how this varies based on the type of centrality measure used. However, LLMs fail to demonstrate centrality and clustering similarity with humans, suggesting that human populations have a distinct internal world model compared to LLM agents.

Our results depend on the vividness ratings for imagined scenes, which quantify the subjective quality of an imagined experience. What does vividness mean for human and LLM responses? The epistemology of vividness remains a topic of debate. Hume in his *Treatise of Human Nature*<sup>59</sup> famously introduced the notion of vividness of experiences as the "force" and "vivacity" of our internal representations, with perception (i.e., externally-generated experiences)

having higher vividness than imagination and memory. Contemporary philosophers, such as Langkau (2021)<sup>60</sup>, have argued that the vividness of imagination can be categorized into two types: the vividness of mental images (reflected by the degree of congruence with externally generated perceptual content) and the vividness of mental experiences (reflected by the intensity of experience). Fazekas (2024) also divides the vividness into subjective intensity and subjective specificity. The intensity of the subjective experience, in terms of vividness, can be domain-general and provide an index of the strength of phenomenological experience<sup>61,62</sup>. Thus, current philosophical research suggests that the vividness of imagination is multidimensional, and certain features can be linguistically specified<sup>60</sup>. Therefore, vividness forms a key psychological descriptor of internal representations with multidimensional characteristics<sup>61</sup>.

Previously, topological geometry was found to be highly similar for color similarity between humans and LLMs<sup>63</sup>. To investigate color similarity, researchers employed supervised and unsupervised algorithms to map the similarity between two topological distributions (Humans and LLMs) of colors based on similarity ratings<sup>63</sup>. Our results suggest that humans and LLMs do not exhibit a similar topological distribution of imagined nodes connected by associations of vividness ratings between them. The difference could be primarily due to theoretical differences in ratings of (dis)similarity and vividness. LLMs can learn the (dis)similarity between words (such as different colors), as their training algorithms incentivize them to learn semantic information from the training datasets<sup>64</sup>. On the other hand, vividness ratings require humans to rely on the strength of their phenomenological experience of an imagined scenario, which can be influenced by other experiences of different scenarios in long-term memory, as presented in imagination networks (Figs. 2 & 3). Critically, humans rely on phenomenological aspects of experience and memory, which results in the vividness of

imagined experiences. Although LLMs possess phenomenological knowledge, their vividness ratings change based on the strength of imagination when prompted with different imagination abilities, as shown in Fig. 1A. Thus, they lack clear phenomenological structures, as indicated by the similarity of centralities and clustering of imagination networks (Figs. 4 and 5). Overall, our results suggest that differences in linguistic capacity and human thought<sup>65,66</sup> are reflected in differences between the internal world models across humans and LLMs in our tasks, specifically in the form of imagination networks. Interestingly, we note that for the PSIQ, prompts for imagination across different sensory modalities showed strongly correlated closeness centrality between humans and several LLMs, which was not the case for the VVIQ, which includes scenarios about general environmental scenes. Thus, some of our evidence indicates that these versions of LLMs are (to a certain degree) more similar to human sensory world models, compared to world models based on experiences. This may have occurred due to more structured knowledge about sensory experiences (compared to general environmental scenes) in the training data, as LLMs lack the experiences that humans acquire by being embedded in the environment.

Previous attempts to characterize internal world models have yielded mixed findings, and definitions of world models have been contingent upon specific task characteristics. For example, some researchers have utilized the map of Manhattan as the base world model to train AI models to navigate between locations within it<sup>67</sup>. Their findings revealed that AI models do not show an implicit map of the world, and that the map could not be recovered from their responses. On the other hand, it has also been demonstrated that LLM-like models exhibit emergent properties, demonstrating their knowledge for unobserved and intermediate stages of the grid world<sup>68</sup>. However, both of these examples lack comparison with human behavior. The contemporary epistemology of the world model is highly task-dependent, specifically in

measuring the relationship between an LLM model's IWM and the control used for the task. Our approach, on the contrary, conceives of a world model as a latent mental phenomenon that can be accessed across different imagination tasks (VVIQ-2 or PSIQ). Our network-based comparative approach does not negate the existence of a world model in LLMs, but rather characterizes the extent of similarity with human world models for LLMs, which is accessed using reproductive imagination vividness reports as imagination networks.

Generalizable findings across measures of centrality (expected influence, strength, and closeness) and clustering alignment reveal that importance of nodes across human populations are distinct from LLMs. As to why this occurs in human populations, this remains a question for future research. It could be due to the presence of similar recovery map<sup>69</sup> in human populations, which is a recently proposed theoretical concept to define world models in reinforcement learning agents. Specifically, in this approach, the IWM is a recovery map computed by approximation of transition states in which an agent is embedded, and describes the changes in the states of the environment after an agent takes an action<sup>69</sup>. Recovery maps characterize an agent's internal world model in which it is embedded, and capture task actions which change the state as approximations of transition states. Since we utilize highly common scenarios for imagination, humans might have similar approximations of transition states (recovery maps) of the commonly imagined scenarios, but the lack of betweenness centrality correlation may indicate individual differences in the recovery map among cognitive agents for the internal world model. Future empirical work will help to disentangle how recovery maps and network measures can both contribute to understanding of IWMs.

As our measurements depend on behavioral vividness ratings, if a population of cognitive agents imagines hyper-realistically, then the vividness ratings may reach the ceiling, and our

approach would not lead to the formation of networks. On the other hand, such a population may suffer from a higher degree of confusion with reality, as reality monitoring often fails for highly vivid imagined experiences<sup>70,71</sup>. Furthermore, our experiments with LLMs induced personas<sup>72</sup> (see Methods) for the imagination prompts, which may not be sufficient to reveal structural regularities in our imagination task for vividness ratings comparable to those of human populations. However, it is not yet known how a persona can be designed that enables LLMs to possess a human-like richness of phenomenological experience, under which LLMs show high similarity to our measurements with humans. We utilized population diversity sampling (see Methods) to diversify simulations from a given LLM agent, aiming to incorporate diversity in imagination abilities, which are often present in human populations. However, we found that the LLM and human cognitive agents exhibit different topological distributions of imagination networks. Thus, imagination's purpose could be to access the recovery map that an agent builds using experiences in the environment instead of reward maximization. Further, our network-based approach presented here presents static structural regularities in world models; although some imagination prompts were about dynamic imagination (e.g. imagination while being in a moving car from VVIQ-2), future research can explore dynamical properties of world models using network based methods using imagination of dynamical experiences<sup>30,73</sup>.

In conclusion, we present one of the first ever direct psychological and cognitive examinations of internal world models across humans and LLMs, using the imagination of everyday environmental scenes and sensory experiences. Our study characterized IWMs as possessing inherent characteristics rooted in the psychology of imagination and network science. We introduced network measures, such as centrality and clustering, to examine the characteristics of world models in humans and LLMs, and showed distinct IWMs across these

two groups. This work lays a foundation for evaluating whether artificial intelligence possesses internal world models similar to those of humans through the use of imagination.

## Methods

### Participants

There were 541 participants (394 females and 147 males) in the VVIQ-2 Florida data, with a mean age of 20.4 years. The Florida dataset for both the VVIQ-2 and PSIQ was curated from responses provided by participants at the University of Florida, who received course credit for completing the task successfully. The data was collected from participants who gave consent prior to the start of the study. The study was approved by the Institutional Review Board of the University of Florida (IRB No.: ET00045024). For the Polish VVIQ-2 data, 1651 participants (1043 females and 608 males) fully completed the questionnaire in the openly available dataset from Jankowska & Karwowski (2022)<sup>51</sup>, which comprises individuals from schools in Poland at the undergraduate level of college. We created two non-overlapping subsets of 600 participants by randomly sampling the Polish dataset as “*Polish 1*” and “*Polish 2*,” whereas “*Polish All*” consists of all the data (1651 participants) from Poland in the results. We also analyzed the data by pooling all the data from the “Florida + Poland” group, which consisted of 2192 individuals.

For the PSIQ, there were 334 participants (276 females and 58 males) from Florida with a mean age of 20.5 years, and these participants also performed the VVIQ-2. There were 217 participants in the London dataset, which is openly available from Clark & Maguire (2023)<sup>52</sup>, with a mean age of 29 years and comprising 109 females and 108 males. We also analyzed the data by pooling all the data from the “Florida + London” group, which comprised 551 participants. For more details on the Polish and London datasets, the readers are advised to look at the Jankowska & Karwowski (2022) and Clark & Maguire (2023) publications, respectively. In each population, participants either performed the VVIQ-2 or the PSIQ questionnaires, as instructed. Polish data was obtained from participants doing the Polish translated version of

VVIQ-2. In contrast, all the other populations performed the imagination surveys in the original English version.

### **AI Models**

We used six models in total, with four from the Gemma3 family and two models from the Llama family. From the Gemma3 family, we utilized models with 12 and 27 billion parameters, along with their corresponding quantization-aware trained models (postfixed as QAT). Quantized models often reduce model size without changing the number of parameters and quality of responses by lowering the decimal precision of the model weights, enabling us to compare models across different training regimes while keeping the model architecture constant. For more information about the quantization-aware training, readers are recommended to refer to Jacob et al., (2017)<sup>74</sup>. From the Llama family, we used Llama-3.3, which has 70 billion parameters, and Llama-4.0-Scout (16x17b), a model that combines an expert's model with 16 experts and 17 billion parameters each. Thus, each model offers a distinct type of long-term memory, based on its training regime and architecture. All models were run locally using one NVIDIA B100 GPU.

### **Imagination Tasks**

The VVIQ-2 and PSIQ ask participants to rate the vividness of their imagination on a scale of 1 to 5 and 0 to 10, respectively, for a given item prompt. We assume that vividness ratings capture a psychological experience based on the perceived vividness of the internal world. The VVIQ-2 consists of eight contexts with four items each with 32 items in total. We used three items in each of the PSIQ's contexts, with 21 total imagination prompts. We hypothesized that the vividness ratings may exhibit structural characteristics due to the internal world model, organized similarly across human populations. However, in the current investigation, we utilized the VVIQ-2 and PSIQ as tools to sample the internal world model

using imagination prompts and vividness ratings, and measure the structural aspects of human and LLM imagination using psychological network science. Inherently, the VVIQ-2 and PSIQ are structurally clustered and organized based on different contexts (8 contexts in VVIQ-2 and 7 contexts in PSIQ, as mentioned above). Additionally, the VVIQ-2 contexts focus solely on the visual aspects of the external world, whereas the PSIQ contexts sample the ability to generate and experience sensory imagery across multiple modalities.

For the simulation of LLM responses, the English version of the imagination questionnaires was converted into JSON format and can be found on the OSF site. AI model providers frequently use JSON to format text for training the LLM models<sup>75</sup>. Using explicit output parsers, our LLMs were constrained to provide only vividness responses, and with our LLM-based AI models, we performed the imagination task in two ways: (1) independently and (2) cumulatively. In the independent condition, LLM models responded to each context and prompt without recalling previous trials, treating each item as independent from the others. During the cumulative condition, LLM models had access to previous interactions and values; thus, only the first item in this condition did not have information about the past, while subsequent items had a memory of past interactions with items/prompts and their own vividness rating. Thus, our two tasks allowed us to simulate vividness ratings with either (1) independence of previous trials, or (2) having previous trial memory, in LLM models for simulation.

The system message to each LLM call was provided in the following format:

{*“You are a helpful assistant with the following individual characteristics:*

*<definition of imagination ability> <persona statements>*

*Perform the task as per the instructions described below.*

*TASK CONTEXT: <instructions>” }*

An example trial for the VVIQ-2 given to the LLM looked like the following:

“{"TRIAL\_CONTEXT": "Think of the rising sun. Consider carefully the picture that comes before your mind's eye.", "TRIAL": "A rainbow appears."}”. The trial context and message changed depending on the questionnaire. An example trial for the PSIQ looked like: "Imagine the appearance of a bonfire. How vivid is the image?"

The instructions in the task context above were similar to the instructions provided to human participants for the imagination questionnaire. The items from the imagination questionnaire were provided as human/user messages with their item context. The item from each questionnaire to the LLM was provided as Human/User messages for the LLMs to provide the vividness rating as responses in JSON format: {Vividness: x}, depending on the scale of the given imagination questionnaire.

Each model was used to simulate 200 personas randomly sampled from the Persona-Chat dataset<sup>72</sup> across five levels of imagination ability characteristics. To simulate different imagination abilities, we manipulated them across five levels: (a) no imagination ability prompt; (b) typical imagery: *“Typical imagery is a standard mental imagery capacity most people have. It allows for moderately vivid and detailed mental pictures. Individuals with typical imagery can summon clear, detailed images in their mind's eye but might not be able to sustain them for long periods or with photographic precision.”*; (c) aphantasia: *“Aphantasia is inability to form mental images, even when attempting to do so. Individuals with aphantasia typically describe a "blank mind's eye" when asked to imagine something, such as a loved one's face or a scene.”*; (d) hypophantasia: *“Hypophantasia is reduced ability to form mental images. Visualizations may exist but are vague, dim, or not detailed. Individuals with hypophantasia may perceive faint or blurry images but lacks the richness and clarity of typical imagery.”*; and (e) hyperphantasia:

*“Hyperphantasia is the ability to form extremely vivid, lifelike mental images that are nearly indistinguishable from actual vision. Individuals with hyperphantasia may report “seeing” images as if they were real, with high detail, colors, and sometimes motion.”* When no imagination ability prompt was given, only the persona statements were provided with the task instructions, as in the VVIQ-2 or PSIQ questionnaire. For the simulations involving all other imagination ability characteristics, persona statements were prefixed to the definition of the imagination ability. Thus, in total, for a type of task (independent or cumulative), 1000 simulations were generated from each LLM model, with 200 simulations for each of the five imagination ability instruction conditions. The total vividness score from the VVIQ-2 was analyzed using JASP (0.19.3) to investigate the effects of LLM task type (cumulative or independent), imagination ability prompt, and model (Fig. 1A). Kruskal-Wallis and Dunn’s post-hoc tests were performed for between-group comparisons, and two-tailed p-values are reported in the Results section. We did not have a hypothesis for the total vividness score, other than anticipating that imagination ability prompts for aphantasia would cause total vividness scores to be lower, and hyperphantasia prompts would cause vividness scores to be higher compared to the typical imagery instruction or no imagination ability instruction.

### **AI Population Diversity Sampling**

For constructing the imagination networks from each of the LLM responses, we created a population of LLM simulations based on human imagination abilities by downsampling 1000 simulations from across imagination abilities to 600 total simulations for each of the LLMs. The human population consists of individuals with varying imagination abilities, as measured using the total vividness score given a questionnaire. We first extracted the quantile ranges using every 10th percentile of the total vividness scores from the pooled human data from the VVIQ-2

(Florida + Poland group) and PSIQ (Florida + London group). For each LLM simulation, given the model and questionnaire, the total vividness score was computed. LLM simulations were selected based on the human quantile ranges, and from each quantile range, 60 LLM simulations were randomly chosen. Whenever there were not enough simulations for a given quantile range, all simulations were selected within the given quantile range. The remaining simulations for that quantile were chosen from outside the quantile range and removed from the overall samples for further sampling. Thus, after population diversity sampling, we had 600 simulations from each of the models for the given task (independent or cumulative) and imagination questionnaire (VVIQ-2 or PSIQ), which were used to create imagination networks.

Additionally, an important reason to perform AI population diversity sampling is that differences in imagination abilities could explain the topological regularities observed in human imagination networks. Diversifying AI simulations based on imagination ability from human data helps us introduce statistical variances for the LLM-based imagination networks, which can represent the distribution of human imagination across different imagination abilities. Total vividness scores for the VVIQ-2 data were analyzed for different populations from human groups and LLM models after population diversity sampling (Fig. 1B) using Kolmogorov-Smirnov (K-S) tests with Benjamini/Hochberg FDR corrections for multiple comparisons, with two-tailed p-values reported.

### **Network Analysis**

By performing network analysis of vividness ratings, we can investigate the internal world model of characterizing how one experiences their environment in day-to-day activities using reproductive imagination. We constructed the edge weights between two nodes (scenes) to represent the associations between them, thus creating an imagination network representing the

internal worlds in the two tasks. Therefore, the node represents the state of the world, and edges represent the association between those states that are solely defined by the imagination in an individual's mind, proposed as imagination networks in the current investigation.

Different network measurements represent how the information is processed in the networks. Given a specific imagination network, we characterized the IWM of a human or AI agent using micro-level network centrality of each node, which reveals the importance of each node in a given network. Although there are numerous centrality measures in network science, we focused on four common psychological network centrality measures: expected influence, strength, closeness, and betweenness<sup>76</sup> using the bootnet library<sup>77</sup> in R. In our study, we correlated the different centralities of nodes of an imagination network with those from all other networks to investigate whether each imagined scenario held similar importance across the various networks for a given imagination questionnaire. If a centrality measure for the nodes in an imagined network correlated with another imagined network, we inferred that the imagined scenario was similarly involved across the networks in the overall topology of imagination networks that represent the internal world model. Thus, a positive high correlation of a centrality measure of nodes across imagination networks indicates that the internal world model is similarly utilized across a given type of imagination network.

We performed post-hoc stability analysis; specifically, we computed the CS-coefficient using the bootnet library with a case-dropping value of 500 and a bootstrap value of 5000 for the centrality measurements to establish their robustness and accuracy. Centrality stability is preferred to be above 0.5, or at least above 0.25<sup>54</sup>. The CS-coefficient (centrality stability) effectively measures the proportion of data that can be eliminated while ensuring, with 95% confidence, that a correlation of at least 0.7 is maintained with the original centrality measures<sup>54</sup>.

See Supplementary Table S1 for VVIQ-2 and Table S2 for PSIQ for CS-coefficient results. We investigated whether positive correlations for centrality measures would emerge due to similar world models between agents, and report pairwise Pearson's  $r$  correlations and one-tailed p-values. Whenever pairwise normality was violated, we provided Spearman's  $\rho$  correlations. Further, we also reported Benjamini/Hochberg FDR corrections for multiple comparisons for the p-values.

The vividness ratings are ordinal scale data for which polychoric partial correlations<sup>54</sup> should be preferred, as they assume a latent distribution underlying the ordinal scale value. However, our initial investigations failed to find stable centrality measures in networks, primarily for the LLMs. Thus, the Spearman method was used for partial correlations in EBICglasso for estimating the imagination networks<sup>54</sup>. To investigate whether nodes had similar influences across networks, depending on the type of centrality measures, we performed pairwise correlations between the centralities of nodes across networks.

To understand how different items are in the data clusters based on the associations of vividness ratings between them, we performed clustering analysis using the walktrap community<sup>56</sup> detection algorithm with the LE method in the EGANet library<sup>55</sup> in R. The similarity in cluster assignments of different nodes across the networks was calculated using the adjusted rand score from the sklearn library<sup>78</sup> in Python. The higher the adjusted rand-score, the higher the clustering alignment across networks

Each network was computed using the bootnet library<sup>77</sup> in the R programming language based on the EBICglasso method with a commonly used common tuning parameter of 0.5 using the vividness ratings for each item. The EBICglasso method promotes fewer connections between network nodes by combining Graphical LASSO and the Extended Bayesian Information

Criterion for model selection (EBICglasso), incorporating partial correlations, which results in fewer false-positive edges in the network compared to networks formed solely using partial correlations<sup>54</sup>. See Table S1, S2 for clustering assignment for each node for VVIQ-2, and PSIQ imagination networks respectively.

### References

1. Drubach, D., Benarroch, E. & Mateen, F. Imagination: its definition, purposes and neurobiology. *Rev. Neurol.* **45**, 353 (2007).
2. Moulton, S. T. & Kosslyn, S. M. Imagining predictions: mental imagery as mental emulation. *Philos. Trans. R. Soc. B Biol. Sci.* **364**, 1273–1280 (2009).
3. Pearson, J. The human imagination: the cognitive neuroscience of visual mental imagery. *Nat. Rev. Neurosci.* **20**, 624–634 (2019).
4. Mguidich, H., Zoudji, B. & Khacharem, A. Does imagination enhance learning? A systematic review and meta-analysis. *Eur. J. Psychol. Educ.* **39**, 1943–1978 (2024).
5. Jones, M. & Wilkinson, S. From Prediction to Imagination. in *The Cambridge Handbook of the Imagination* (ed. Abraham, A.) 94–110 (Cambridge University Press, Cambridge, 2020). doi:10.1017/9781108580298.007.
6. Klein, S. B., Robertson, T. E. & Delton, A. W. Facing the future: Memory as an evolved system for planning future acts. *Mem. Cognit.* **38**, 13–22 (2010).
7. Schacter, D. L. *et al.* The Future of Memory: Remembering, Imagining, and the Brain. *Neuron* **76**, 677–694 (2012).
8. Goddu, M. K. & Gopnik, A. The development of human causal learning and reasoning. *Nat. Rev. Psychol.* **3**, 319–339 (2024).
9. Magid, R. W., Sheskin, M. & Schulz, L. E. Imagination and the generation of new ideas. *Cogn. Dev.* **34**, 99–110 (2015).
10. Kidd, C. & Hayden, B. Y. The psychology and neuroscience of curiosity. *Neuron* **88**, 449–460 (2015).

11. Sergeant-Perthuis, G., Ruet, N., Rudrauf, D., Ognibene, D. & Tisserand, Y. Influence of the Geometry of the world model on Curiosity Based Exploration. Preprint at <https://doi.org/10.48550/arXiv.2304.00188> (2023).
12. Clement, C. A. & Falmagne, R. J. Logical reasoning, world knowledge, and mental imagery: Interconnections in cognitive processes. *Mem. Cognit.* **14**, 299–307 (1986).
13. Knauff, M. & May, E. Mental imagery, reasoning, and blindness. *Q. J. Exp. Psychol.* **59**, 161–177 (2006).
14. Myers, J. Reasoning with imagination. in *Epistemic uses of imagination* 103–121 (Routledge, 2021).
15. Douville, P. & Pugalee, D. K. Investigating the relationship between mental imaging and mathematical problem solving. in *Proceedings of the international conference of Mathematics Education into the 21st century project, September 2003* 62–67 (2003).
16. Angell, J. R. *Psychology: An Introductory Study of the Structure and Function of Human Consciousness*. (H. Holt, 1908).
17. Silver, D. *et al.* Mastering the game of Go without human knowledge. *Nature* **550**, 354–359 (2017).
18. Silver, D., Singh, S., Precup, D. & Sutton, R. S. Reward is enough. *Artif. Intell.* **299**, 103535 (2021).
19. Silver, D. & Veness, J. Monte-Carlo Planning in Large POMDPs. in *Advances in Neural Information Processing Systems* (eds Lafferty, J., Williams, C., Shawe-Taylor, J., Zemel, R. & Culotta, A.) vol. 23 (Curran Associates, Inc., 2010).
20. Eppe, M. *et al.* Intelligent problem-solving as integrated hierarchical reinforcement learning. *Nat. Mach. Intell.* **4**, 11–20 (2022).

21. Lin, Y.-C. *et al.* MIRA: Mental Imagery for Robotic Affordances. in *Proceedings of The 6th Conference on Robot Learning* 1916–1927 (PMLR, 2023).
22. Matsuo, Y. *et al.* Deep learning, reinforcement learning, and world models. *Neural Netw.* **152**, 267–275 (2022).
23. Racanière, S. *et al.* Imagination-Augmented Agents for Deep Reinforcement Learning. in *Advances in Neural Information Processing Systems* vol. 30 (Curran Associates, Inc., 2017).
24. Weber, T. *et al.* Imagination-Augmented Agents for Deep Reinforcement Learning. *arXiv.org* <https://arxiv.org/abs/1707.06203v2> (2017).
25. Wu, W. *et al.* Mind’s Eye of LLMs: Visualization-of-Thought Elicits Spatial Reasoning in Large Language Models. in (2024).
26. Gershman, S. J., Zhou, J. & Kommer, C. Imaginative Reinforcement Learning: Computational Principles and Neural Mechanisms. *J. Cogn. Neurosci.* **29**, 2103–2113 (2017).
27. Smieja, J. M., Zaleskiewicz, T. & Gasiorowska, A. Mental imagery shapes emotions in people’s decisions related to risk taking. *Cognition* **257**, 106082 (2025).
28. Zaleskiewicz, T., Bernady, A. & Traczyk, J. Entrepreneurial Risk Taking Is Related to Mental Imagery: A Fresh Look at the Old Issue of Entrepreneurship and Risk. *Appl. Psychol.* **69**, 1438–1469 (2020).
29. Zaleskiewicz, T., Traczyk, J. & Sobkow, A. Decision making and mental imagery: A conceptual synthesis and new research directions. *J. Cogn. Psychol.* **35**, 603–633 (2023).
30. Balaban, H. & Ullman, T. D. The capacity limits of moving objects in the imagination. *Nat. Commun.* **16**, 5899 (2025).
31. Abraham, A. The imaginative mind. *Hum. Brain Mapp.* **37**, 4197–4211 (2016).

32. Abraham, A. & Bubic, A. Semantic memory as the root of imagination. *Front. Psychol.* **6**, (2015).
33. Mahadevan, S. Imagination Machines: A New Challenge for Artificial Intelligence. *Proc. AAAI Conf. Artif. Intell.* **32**, (2018).
34. Addis, D. R., Pan, L., Vu, M.-A., Laiser, N. & Schacter, D. L. Constructive episodic simulation of the future and the past: Distinct subsystems of a core brain network mediate imagining and remembering. *Neuropsychologia* **47**, 2222–2238 (2009).
35. Schacter, D. L. & Addis, D. R. The cognitive neuroscience of constructive memory: remembering the past and imagining the future. *Philos. Trans. R. Soc. B Biol. Sci.* **362**, 773–786 (2007).
36. Schacter, D. L., Addis, D. R. & Buckner, R. L. Episodic simulation of future events: Concepts, data, and applications. *Ann. N. Y. Acad. Sci.* **1124**, 39–60 (2008).
37. Hassabis, D., Kumaran, D. & Maguire, E. A. Using imagination to understand the neural basis of episodic memory. *J. Neurosci.* **27**, 14365–14374 (2007).
38. Hassabis, D. & Maguire, E. A. Deconstructing episodic memory with construction. *Trends Cogn. Sci.* **11**, 299–306 (2007).
39. Schacter, D. L. & Addis, D. R. On the constructive episodic simulation of past and future events. *Behav. Brain Sci.* **30**, 331–332 (2007).
40. Schacter, D. L., Benoit, R. G. & Szpunar, K. K. Episodic future thinking: mechanisms and functions. *Curr. Opin. Behav. Sci.* **17**, 41–50 (2017).
41. Spagna, A. *et al.* Visual mental imagery: Evidence for a heterarchical neural architecture. *Phys. Life Rev.* **48**, 113–131 (2024).

42. Spagna, A. *et al.* Competing models of visual mental imagery: Reverse hierarchy or heterarchy? *Phys. Life Rev.* **51**, 96–100 (2024).
43. Ranjan, S. & Odegaard, B. Heterarchy or hierarchy? Insights from a new model of visual imagination. *Phys. Life Rev.* **49**, 74–76 (2024).
44. Casto, C., Ivanova, A., Fedorenko, E. & Kanwisher, N. What does it mean to understand language? *ArXiv Prepr. ArXiv251119757* (2025).
45. Schwarzkopf, D. S. *et al.* Vividness of mental imagery is a broad trait measure of internally generated visual experiences. 2025.09.30.679629 Preprint at <https://doi.org/10.1101/2025.09.30.679629> (2025).
46. Marks, D. F. New directions for mental imagery research. *J. Ment. Imag.* **19**, 153–167 (1995).
47. Andrade, J., May, J., Deeptose, C., Baugh, S.-J. & Ganis, G. Assessing vividness of mental imagery: The Plymouth Sensory Imagery Questionnaire. *Br. J. Psychol.* **105**, 547–563 (2014).
48. Sumers, T. R., Yao, S., Narasimhan, K. & Griffiths, T. L. Cognitive Architectures for Language Agents. Preprint at <https://doi.org/10.48550/arXiv.2309.02427> (2024).
49. Andreas, J. Language Models as Agent Models. Preprint at <https://doi.org/10.48550/arXiv.2212.01681> (2022).
50. Wang, S. L., Isola, P. & Cheung, B. Words That Make Language Models Perceive. Preprint at <https://doi.org/10.48550/arXiv.2510.02425> (2025).
51. Jankowska, D. M. & Karwowski, M. How Vivid Is Your Mental Imagery? *Eur. J. Psychol. Assess.* **39**, 437–448 (2023).

52. Clark, I. A. & Maguire, E. A. Release of cognitive and multimodal MRI data including real-world tasks and hippocampal subfield segmentations. *Sci. Data* **10**, 540 (2023).
53. Hubert, L. & Arabie, P. Comparing partitions. *J. Classif.* **2**, 193–218 (1985).
54. Epskamp, S. & Fried, E. I. A tutorial on regularized partial correlation networks. *Psychol. Methods* **23**, 617–634 (2018).
55. Golino, H. & Christensen, A. *EGAnet: Exploratory Graph Analysis – A Framework for Estimating the Number of Dimensions in Multivariate Data Using Network Psychometrics*. (2025). doi:10.32614/CRAN.package.EGAnet.
56. Pons, P. & Latapy, M. Computing communities in large networks using random walks. in *International symposium on computer and information sciences* 284–293 (Springer, 2005).
57. Fortunato, S. Community detection in graphs. *Phys. Rep.* **486**, 75–174 (2010).
58. Bringmann, L. F. *et al.* What do centrality measures measure in psychological networks? *J. Abnorm. Psychol.* **128**, 892–903 (2019).
59. Hume, D. *A Treatise of Human Nature*. (Oxford University Press, Oxford, 2009).
60. Langkau, J. Two Kinds of Imaginative Vividness. *Can. J. Philos.* **51**, 33–47 (2021).
61. Fazekas, P. Vividness and content. *Mind Lang.* **39**, 61–79 (2024).
62. Morales, J. Mental strength: A theory of experience intensity. *Philos. Perspect.* **37**, 248–268 (2023).
63. Kawakita, G., Zeleznikow-Johnston, A., Tsuchiya, N. & Oizumi, M. Gromov–Wasserstein unsupervised alignment reveals structural correspondences between the color similarity structures of humans and large language models. *Sci. Rep.* **14**, 15917 (2024).
64. Pezzulo, G., Parr, T., Cisek, P., Clark, A. & Friston, K. Generating meaning: active inference and the scope and limits of passive AI. *Trends Cogn. Sci.* **28**, 97–112 (2024).

65. Fedorenko, E. & Varley, R. Language and thought are not the same thing: evidence from neuroimaging and neurological patients: Language versus thought. *Ann. N. Y. Acad. Sci.* **1369**, 132–153 (2016).
66. Mahowald, K. *et al.* Dissociating language and thought in large language models. *Trends Cogn. Sci.* **28**, 517–540 (2024).
67. Vafa, K., Chen, J. Y., Rambachan, A., Kleinberg, J. & Mullainathan, S. Evaluating the world model implicit in a generative model. *Adv. Neural Inf. Process. Syst.* **37**, 26941–26975 (2024).
68. Jin, C. & Rinard, M. Emergent representations of program semantics in language models trained on programs. in *Forty-first International Conference on Machine Learning* (2024).
69. Richens, J., Abel, D., Bellot, A. & Everitt, T. General agents contain world models. Preprint at <https://doi.org/10.48550/arXiv.2506.01622> (2025).
70. Gonsalves, B. *et al.* Neural Evidence That Vivid Imagining Can Lead to False Remembering. *Psychol. Sci.* **15**, 655–660 (2004).
71. Dijkstra, N. & Fleming, S. M. Subjective signal strength distinguishes reality from imagination. *Nat. Commun.* **14**, 1627 (2023).
72. Zhang, S. *et al.* Personalizing Dialogue Agents: I have a dog, do you have pets too? in *Proceedings of the 56th Annual Meeting of the Association for Computational Linguistics (Volume 1: Long Papers)* (eds Gurevych, I. & Miyao, Y.) 2204–2213 (Association for Computational Linguistics, Melbourne, Australia, 2018). doi:10.18653/v1/P18-1205.
73. Singhal, I. & Srivastava, N. Dynamics of mental imagery. *Conscious. Cogn.* **131**, 103865 (2025).

74. Jacob, B. *et al.* Quantization and Training of Neural Networks for Efficient Integer-Arithmetic-Only Inference. Preprint at <https://doi.org/10.48550/arXiv.1712.05877> (2017).
75. He, J. *et al.* Does Prompt Formatting Have Any Impact on LLM Performance? Preprint at <https://doi.org/10.48550/arXiv.2411.10541> (2024).
76. Borsboom, D. *et al.* Network analysis of multivariate data in psychological science. *Nat. Rev. Methods Primer* **1**, 1–18 (2021).
77. Epskamp, S. & Fried, E. I. Package ‘bootnet’. (2025).
78. [Buitinck, L. \*et al.\* API design for machine learning software: experiences from the scikit-learn project. in \*ECML PKDD Workshop: Languages for Data Mining and Machine Learning\* 108–122 \(2013\).](#)

Supplementary Material

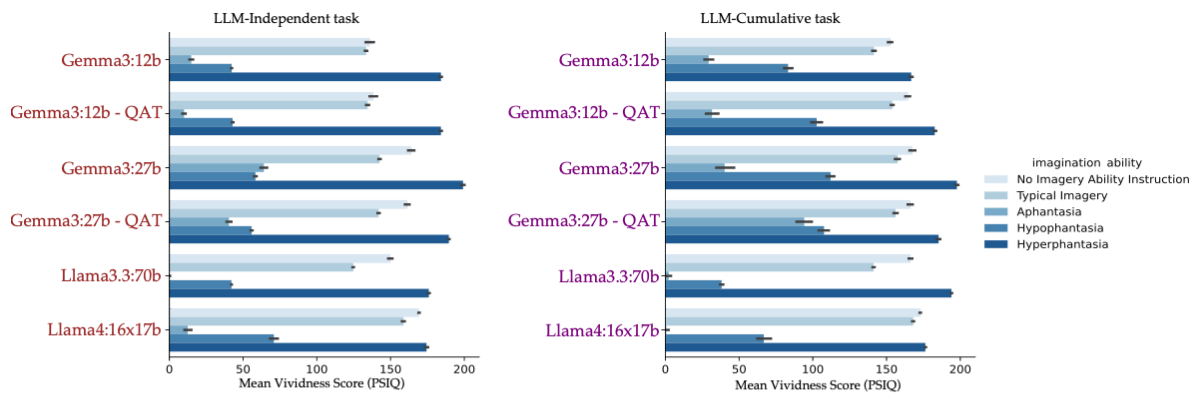
Internal World Models as Imagination Networks in Cognitive Agents

Saurabh Ranjan and Brian Odegaard

Department of Psychology, University of Florida

Address correspondence to: [ranjan.saurabh@outlook.com](mailto:ranjan.saurabh@outlook.com), [bodegaard@ufl.edu](mailto:bodegaard@ufl.edu)

A. LLM's mean vividness across imagination ability.



B. Mean (left) and distribution (right) of total vividness score in Humans and after population diversity sampling in LLMs.

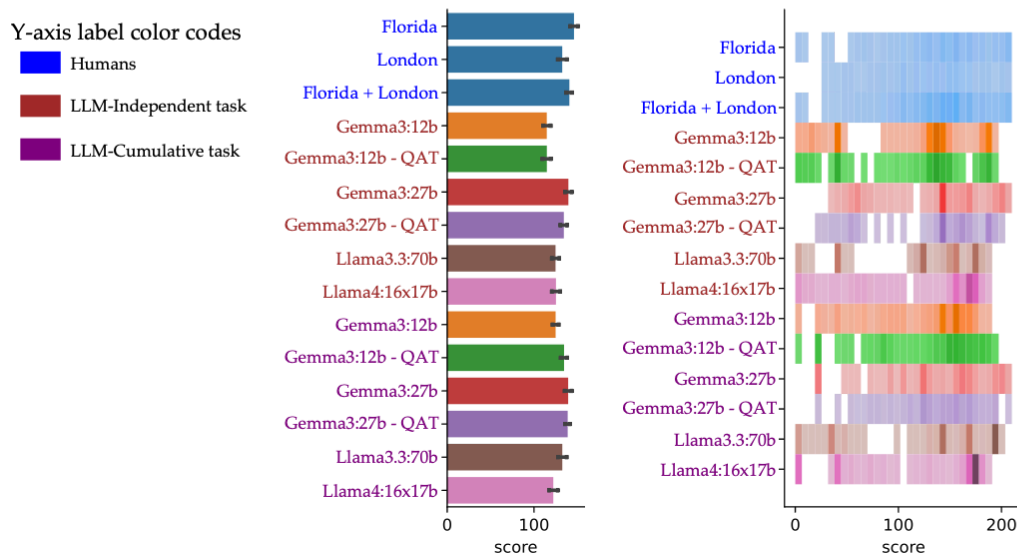


**Fig. S1. Total vividness scores and distributions in LLMs and Humans using the PSIQ.** (A) Total vividness score with prompt about different imagination ability statements on the LLM simulation for PSIQ. (B) (Left) Mean vividness scores in human populations and after population diversity sampling (*see methods*) for each of the LLMs based on the total vividness score of the simulations for PSIQ. (Right) Distribution of the total vividness score in humans and after population diversity sampling for each of the LLMs for PSIQ. The error bars in bar plots are bootstrapped ( $N = 1000$ ) 95% confidence intervals.

**Table S1. CS-Coefficient of nodes for VVIQ-2 imagination networks in different cognitive agents.**

Groups	Betweenness	Closeness	Expected Influence	Strength
Florida	0.42	0.47	0.69	0.57
Poland 1	0.21	0.48	0.71	0.71
Poland 2	0.27	0.45	0.75	0.75
Poland All	0.29	0.52	0.75	0.75
Florida +Poland	0.43	0.73	0.75	0.75
Gemma3:12b_i	0.42	0.42	0.75	0.68
Gemma3:12b-QAT_i	0.18	0.27	0.75	0.75
Gemma3:27b_i	0.21	0.44	0.75	0.75
Gemma3:27b-QAT_i	0.19	0.32	0.75	0.73
Llama3.3:70b_i	0.18	0.31	0.75	0.75
Llama4:16x17b_i	0.39	0.6	0.75	0.65
Gemma3:12b_c	0.39	0.61	0.75	0.67
Gemma3:12b-QAT_c	0.63	0.38	0.75	0.72
Gemma3:27b_c	0.49	0.6	0.75	0.65
Gemma3:27b-QAT_c	0.19	0.32	0.75	0.73
Llama3.3:70b_c	0.44	0.48	0.75	0.75
Llama4:16x17b_c	0.55	0.74	0.75	0.75

Note: CS-Coefficient should ideally be more than 0.50 or at least 0.25 (Epskamp & Fried, 2018). Values are rounded to two decimal places. The postfixes “\_i” and “\_c” to LLM models denote LLM-independent and LLM-Cumulative tasks, respectively.

**Table S2. CS-Coefficient of nodes for PSIQ imagination networks in different cognitive agents.**

Groups	Betweenness	Closeness	Expected Influence	Strength
Florida	0.08	0.4	0.66	0.58
London	0	0.18	0.63	0.45
Florida+London	0.2	0.68	0.75	0.72
Gemma3:12b_i	0.35	0.43	0.75	0.75
Gemma3:12b-QAT_i	0.42	0.35	0.74	0.73
Gemma3:27b_i	0.49	0.74	0.75	0.74
Gemma3:27b-QAT_i	0.33	0.66	0.75	0.74
Llama3.3:70b_i	0.42	0.49	0.75	0.75
Llama4:16x17b_i	0.25	0.61	0.75	0.74
Gemma3:12b_c	0.62	0.64	0.75	0.75
Gemma3:12b-QAT_c	0.14	0.57	0.75	0.75
Gemma3:27b_c	0.58	0.71	0.75	0.68
Gemma3:27b-QAT_c	0.49	0.74	0.75	0.74
Llama3.3:70b_c	0.56	0.58	0.75	0.74
Llama4:16x17b_c	0.25	0.31	0.75	0.29

Note: CS-Coefficient should ideally be more than 0.50 or at least 0.25 (Epskamp & Fried, 2018). Values are rounded to two decimal places. The postfixes “\_i” and “\_c” to LLM models denote LLM-independent and LLM-Cumulative tasks, respectively.



**Table S5. Cluster alignment of nodes for VVIQ-2 imagination networks in different cognitive agents using adjusted rand index (ARI).**

Groups	Florida	Poland-1	Poland-2	Poland-All	Florida + Poland	Gemma3:12_i	Gemma3:12-QAT_i	Gemma3:27_i	Gemma3:27-QAT_i	Llama3.3:70_b_i	Llama4:16x1_7b_i	Gemma3:12_c	Gemma3:12-QAT_c	Gemma3:27_c	Gemma3:27-QAT_c	Llama3.3:70_b_c	Llama4:16x1_7b_c
Florida	1					0	0	0	0	0	0.157068	0.016157	0	0.007047	0.121667	0	0.20064
Poland-1	0.285951	1				0	0	0	0	0	0.205748	0.132181	0	0.05317	0.105831	0	0.104084
Poland-2	0.402658	0.548929	1			0	0	0	0	0	0.201618	0.223963	0	0.029583	0.155482	0	0.145438
Poland-All	0.266272	0.559838	0.56338	1		0	0	0	0	0	0.216749	0.23624	0	0.109957	0.174556	0	0.141407
Florida + Poland	0.389664	0.752988	0.791019	0.750549	1	0	0	0	0	0	0.225974	0.169722	0	0.07227	0.148072	0	0.163799
Gemma3:12_i	0	0	0	0	0	1	1	1	1	1	0	0	1	0	0	1	0
Gemma3:12-QAT_i	0	0	0	0	0	1	1	1	1	1	0	0	1	0	0	1	0
Gemma3:27_i	0	0	0	0	0	1	1	1	1	1	0	0	1	0	0	1	0
Gemma3:27-QAT_i	0	0	0	0	0	1	1	1	1	1	0	0	1	0	0	1	0
Llama3.3:70b_i	0	0	0	0	0	1	1	1	1	1	0	0	1	0	0	1	0
Llama4:16x17b_i	0.157068	0.205748	0.201618	0.216749	0.225974	0	0	0	0	0	1	0.104965	0	-0.015945	0.020942	0	0.124922
Gemma3:12_c	0.016157	0.132181	0.223963	0.23624	0.169722	0	0	0	0	0	0.104965	1	0	0.119578	0.350067	0	0.120743
Gemma3:12-QAT_c	0	0	0	0	0	1	1	1	1	1	0	0	1	0	0	1	0
Gemma3:27_c	0.007047	0.05317	0.029583	0.109957	0.07227	0	0	0	0	0	-0.015945	0.119578	0	1	0.165919	0	-0.00623
Gemma3:27-QAT_c	0.121667	0.105831	0.155482	0.174556	0.148072	0	0	0	0	0	0.020942	0.350067	0	0.165919	1	0	0.072276
Llama3.3:70b_c	0	0	0	0	0	1	1	1	1	1	0	0	1	0	0	1	0
Llama4:16x17b_c	0.20064	0.104084	0.145438	0.141407	0.163799	0	0	0	0	0	0.124922	0.120743	0	-0.00623	0.072276	0	1

Note: Computed pairwise for each imagination network. The above matrix is symmetrical across the diagonal. The postfixes “\_i” and “\_c” to LLM models denote LLM-Independent and LLM-Cumulative tasks, respectively.

**Table S6. Cluster alignment of nodes for PSIQ based imagination networks in different cognitive agents using adjusted rand index (ARI).**

Groups	Florida	London	Florida + London	Gemma3:12_i	Gemma3:12-QAT_i	Gemma3:27_i	Gemma3:27-QAT_i	Llama3.3:70_b_i	Llama4:16x1_7b_i	Gemma3:12_c	Gemma3:12-QAT_c	Gemma3:27_c	Gemma3:27-QAT_c	Llama3.3:70_b_c	Llama4:16x1_7b_c
Florida	1	0.869888	1	0	0	0	0	0	0	0	0	0	0	0.541547	0
London	0.869888	1	0.869888	0	0	0	0	0	0	0	0	0	0	0.450402	0
Florida+London	1	0.869888	1	0	0	0	0	0	0	0	0	0	0	0.541547	0
Gemma3:12_i	0	0	0	1	1	1	1	1	1	1	1	1	1	0	1
Gemma3:12-QAT_i	0	0	0	1	1	1	1	1	1	1	1	1	1	0	1
Gemma3:27_i	0	0	0	1	1	1	1	1	1	1	1	1	1	0	1
Gemma3:27-QAT_i	0	0	0	1	1	1	1	1	1	1	1	1	1	0	1
Llama3.3:70b_i	0	0	0	1	1	1	1	1	1	1	1	1	1	0	1
Llama4:16x17b_i	0	0	0	1	1	1	1	1	1	1	1	1	1	0	1
Gemma3:12_c	0	0	0	1	1	1	1	1	1	1	1	1	1	0	1
Gemma3:12-QAT_c	0	0	0	1	1	1	1	1	1	1	1	1	1	0	1
Gemma3:27_c	0	0	0	1	1	1	1	1	1	1	1	1	1	0	1
Gemma3:27-QAT_c	0.541547	0.450402	0.541547	0	0	0	0	0	0	0	0	0	0	1	0
Llama3.3:70b_c	0	0	0	1	1	1	1	1	1	1	1	1	1	0	1
Llama4:16x17b_c	0	0	0	1	1	1	1	1	1	1	1	1	1	0	1

Note: Computed pairwise for each imagination network. The above matrix is symmetrical across the diagonal. The postfixes “\_i” and “\_c” to LLM models denote LLM-Independent and LLM-Cumulative tasks, respectively.